Chapter 4
Causal Bond Graphs and Forms of Mathematical Models

4.1 Causal Paths Between Resistive Ports

After the discussion of the systematic construction of bond graphs, their causal augmentation and the systematic derivation of equations from a causal bond graph, we are prepared to consider different causal patterns in bond graphs and their relation with different forms of mathematical models in detail.

As a general prerequisite, we assume that if controlled sources appear in a bond graph, their modulating signal can be expressed by system inputs or by state variables. Furthermore, if transformers and gyrators are modulated, they are allowed to be modulated only by state variables. The reason for this confinement is that otherwise, algebraic loops may result that are not easily detected by inspection of a causal bond graph as will be explained in more detail in Section 4.8.

In Chapter 5, approaches to the symbolic and numerical solution of mathematical models derived from bond graphs are considered in detail [4, 5].

It has already been pointed out in the previous chapter that a causally completed bond graph gives indication to the form of a mathematical model prior to any equations formulation. In that context, the notion of a *causal path* plays an important role (Definition 3.5). The simplest case of bond graphs has already been dealt with. That is, all storage ports have preferred integral causality. There are neither causal paths between resistive ports, nor causal loops, nor causal meshes in the junction structure. In this case, the equations derived from the bond graph can be written in state space form.

In the following, relaxations of these conditions will be considered. First, causal paths between resistive ports are allowed as they result in bond graphs, e.g., of electrical or hydraulic Wheatstone bridges. Figure 4.1 shows a hydraulic bridge circuit with variable area orifices and a symmetric double acting cylinder in the load diagonal. The piston has a cross sectional area A and a mass m. The transformation of the circuit schematic into a bond graph is straightforward. Choosing the return pressure of the reservoir, p_T, as a reference results in the bond graph depicted in Figure 4.2. The annotations $g_i()$ of the resistor symbols denote a nonlinear function

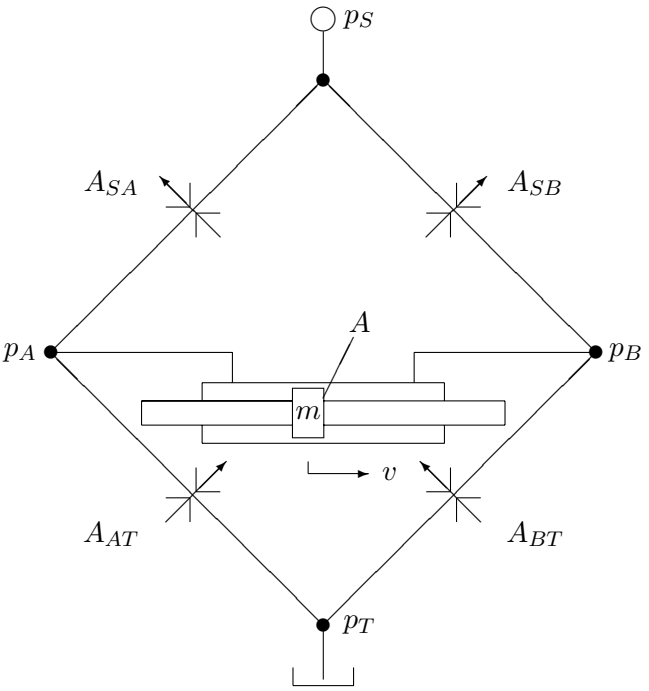

Fig. 4.1 Hydraulic Wheatstone bridge with a symmetric double acting cylinder in the load diagonal

relating the pressure drop across the orifice to the volume flow through the orifice according to Bernoulli's law. Since the example is a hydraulic circuit, power variables are denoted by the symbol 'p' (pressure) and 'Q' (volume flow), as common in hydraulics. The bond graph of Figure 4.2 shows two disjoint causal paths between the resistive ports with bonds enumerated $1-2-3$ and $4-5-6$.

If the outputs of the resistors R_i are denoted p_i or Q_i depending on their causality, then the following set of equations can be derived from the bond graph of Figure 4.2.

$$p_S = f_S(t) \tag{4.1a}$$
$$p_1 = g_1^{-1}\,(\,Q_2 \,-\, A\,v\,) \tag{4.1b}$$
$$Q_2 = g_2\,(\,p_S \,-\, p_1\,) \tag{4.1c}$$
$$Q_3 = g_3\,(\,p_S \,-\, p_4\,) \tag{4.1d}$$
$$p_4 = g_4^{-1}\,(\,Q_3 \,+\, A\,v\,) \tag{4.1e}$$
$$\dot{v} = \frac{1}{m}\,[\,(\,p_S \,-\, p_4\,) \,-\, (\,p_S \,-\, p_1\,)\,] \tag{4.1f}$$

The system of algebraic equations for the outputs of the four resistors is divided into two separate subsystems with two coupled equations because the two causal paths

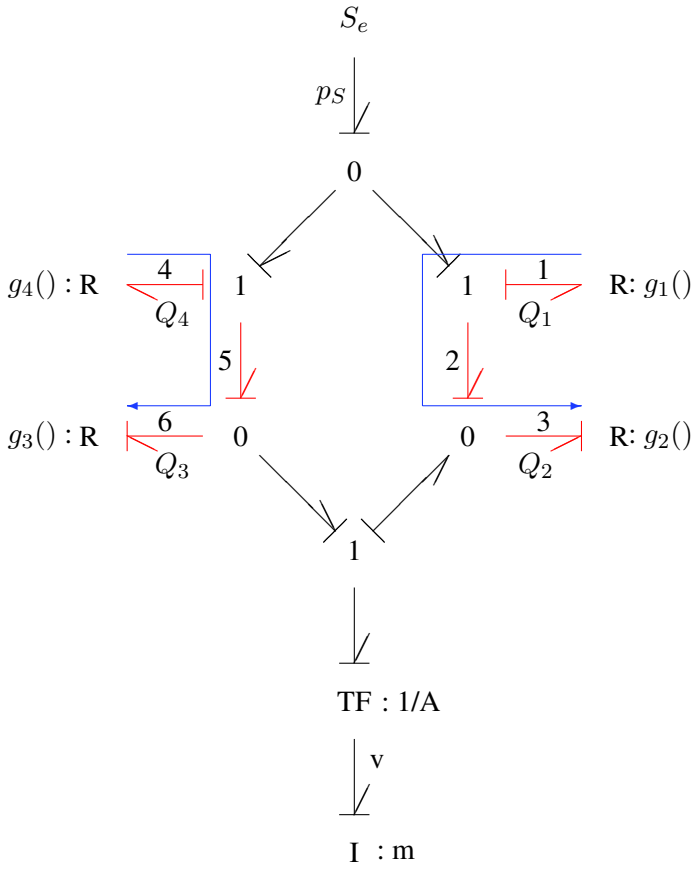

Fig. 4.2 Bond graph of the hydraulic bridge with two disjoint causal paths between resistive ports

are disjoint. Two of the four algebraic unknowns belong to one subsystem, while the other two belong to the other. Variables p_1 and Q_2 both belong to the causal path with bonds labelled $1-2-3$. The corresponding Equations 4.1b and 4.1c may be graphically represented as a signal flow loop along the causal path $1-2-3$. Consider the signal flow loop along the causal path $1-2-3$. The volume flow Q_2 enters into resistor 1. The pressure p_1 leaving that resistor is an input into resistor 2, while the volume flow Q_2 is an output of resistor 2. That is, both power variables of each bond of the causal path are involved in the signal flow loop. This gives rise to the following definitions.

Definition 4.1 (*Topological loop*)**.** A topological loop is a signal flow loop along a causal path or a causal loop. The causal path must not begin or end at an ideal source.

Remark 4.1. A causal path that begins or ends at an ideal source is not associated with a topological loop because the power port variables of an ideal source or sink are not related. In other words, an ideal source breaks a topological loop.

Definition 4.2 (*Topological path*)**.** A topological path is a part of a topological loop. It is a signal flow graph fragment that represents bond variables and constitutive relations being part of a causal path.

Definition 4.3 (*Algebraic loop*)**.** If the variables of a topological loop depend *algebraically* on themselves, that is no integration with respect to time is involved, then the topological loop is called an *algebraic loop*.

Definition 4.4 (*Order of a topological loop*)**.** The order of a topological loop denotes the number of remaining integrators involved in the causal path. If there is no remaining integration in the causal path, then the topological loop is called a zero-order loop.

Definition 4.5 (*Flat loop*)**.** A topological loop is called a *flat loop* if both opposite signals of each bond being part of the causal path or causal loop are involved in the signal flow loop.

Remark 4.2. A flat loop passes each bond of the causal path or causal loop twice.

Figure 4.3 depicts a flat loop related with the causal path $1 - 2 - 3$.

Definition 4.6 (*Open loop*)**.** A topological loop that uses only one of the opposite signals of some or all bonds in a causal path is called an *open loop*.

Remark 4.3. Prerequisite for an open loop is a bond loop. (Definition 3.7).

The topological loop in Figure 4.4 only uses one of the two power variables of the bonds involved in the bond loop. Hence, according to the above definition, it is an open loop. There is a second open loop not depicted in the graph that runs in parallel to the first, but is oppositely oriented. The places where the signal path that leaves

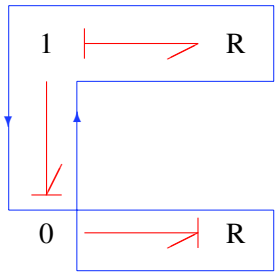

Fig. 4.3 Flat loop related with a causal path

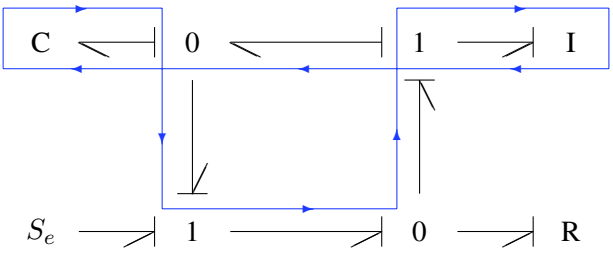

Fig. 4.4 Example of an open loop with mesh stubs

the bond loop reverses in a 1-port passive element and returns into the bond loop are called *mesh stubs* [10].

In [10], Brown observes:

> Most loops in passive systems are flat, and in fact a tree-like bond graph (with no meshes) cannot have other than flat loops.

The topological loops in the bond graph of the example are parts of a signal flow graph that can be assigned to the bond graph. This link between bond graphs and signal flow graphs will be considered later in Chapter 6 in more detail. In this chapter, it sufficient to note that a causal path between two resistive ports indicates an algebraic loop.

In the example under consideration, the causal paths do not touch. Thus, for each of the two causal paths, we can substitute one of the algebraic equations into the other one. As a result, we obtain two implicit algebraic equations that can be separately solved. With the solutions of the two equations the other unknown can be directly computed. In Section 5.4, we will consider the case in which causal paths share bonds and introduce an approach leading to a small set of coupled equations. Once its solution is known, all other algebraic unknowns can be directly computed.

In [32], van Dijk introduces several classes of causal paths depending on the type of ports they connect or whether they are closed. He calls causal paths between resistive ports *class-2 zero-order causal paths*. The prefix *zero-order* emphasises that the variables of the causal path are algebraically coupled.

If the outputs of the resistors in the bond graph of Figure 4.2 are combined into an auxiliary vector $\mathbf{h} = (p_1, Q_2, p_4, Q_3)^T$, then the equations of the example may be written in the general form

$$\mathbf{h}(t) = \mathbf{f}_1(\,\mathbf{x}(t), \mathbf{h}(t), \mathbf{u}(t)\,) \tag{4.2a}$$

$$\dot{\mathbf{x}}(t) = \mathbf{f}_2(\,\mathbf{x}(t), \mathbf{h}(t), \mathbf{u}(t)\,) \tag{4.2b}$$

with $\mathbf{x} = [v]$ and $\mathbf{u} = [p_S]$.

The causal paths in the bond graph of Figure 4.2 indicate that the standard Sequential Causality Assignment Procedure (SCAP) requires an inversion of the characteristic of two of the four resistors, which is possible in this case. In the case of

non-invertible characteristics, the causalities at two resistive ports would not agree with the form of the constitutive equations. We could account for non-invertible resistor characteristics by writing Equations 4.1b and 4.1e in the form

$$g_1\,(p_1) = Q_2 \;-\; A\,v \tag{4.3a}$$
$$g_4\,(p_4) = Q_3 \;+\; A\,v\,, \tag{4.3b}$$

leading to a semi-explicit nonlinear DAE system of the general form

$$\mathbf{0} = \tilde{\mathbf{f}}_1(\,\mathbf{x}(t), \mathbf{h}(t), \mathbf{u}(t)\,) \tag{4.4a}$$
$$\dot{\mathbf{x}}(t) = \mathbf{f}_2(\,\mathbf{x}(t), \mathbf{h}(t), \mathbf{u}(t)\,)\;. \tag{4.4b}$$

We will consider another causality assignment procedure in addition to the standard Sequential Causality Assignment Procedure (SCAP) used so far. It is the method of *relaxed* causalities as introduced by Joseph and Martens (cf. Section 4.9).

4.2 Some Fundamentals from the Theory of Differential-Algebraic Systems

Figure 4.2 of the previous example illustrates that the mathematical model derived from a bond graph takes the form of a DAE system if there are causal paths between resistive ports. An essential characteristic of DAE systems is their so-called *index*. To put it simply, it is an indication of how far away a DAE system is from an ODE system. An early 1982 article by Petzold [27] considering some of the difficulties that can occur with the numerical solution of DAE systems is titled:

> Differential/Algebraic Equations are not ODEs

A general experience is that the higher the index is, the more difficulties are to be expected with the numerical solution of the DAE system (see Section 5.1 and Section 5.5).

Regarding the index of a DAE system, some definitions are required. By providing them, we will follow the presentation in the fundamental book of Brenan, Campbell and Petzold [8]. In the very first sentence of the preface, the authors point out that:

> Differential-algebraic equations (DAE's) arise naturally in many applications, but present numerical and analytical difficulties which do not occur with ordinary differential equations.

Some books on DAE systems are, e.g. [16–18].

In the following, we assume a linear differential-algebraic set of equations of the form

$$\mathbf{A}\,\dot{\mathbf{x}}(t) \;+\; \mathbf{B}\,\mathbf{x}(t) \;=\; \mathbf{f}(t)\;. \tag{4.5}$$

In Equation 4.5, $\mathbf{A}, \mathbf{B}$ are $n \times n$ matrices with constant coefficients, $\mathbf{f} : \mathbb{R} \to \mathbb{R}$ is a vector function of the system inputs and $t \in [0, \infty)$.

Definition 4.7 (*Matrix pencil*)**.** Let $\lambda \in \mathbb{C}$, then $\lambda\mathbf{A} + \mathbf{B}$ is called a *matrix pencil*.

If the determinant $\det(\lambda\mathbf{A} + \mathbf{B})$ is not identically zero as a function of λ, then the matrix pencil is called *regular*.

Remark 4.4. The definition of a regular matrix pencil is important because it is a necessary and sufficient condition for the solvability of a linear constant coefficient DAE (Equation 4.5). ([8], Theorem 2.3.1)

Definition 4.8 (*Index of a matrix*)**.** A quadratic matrix $\mathbf{M}$ is called *nilpotent* if there is positive integer k such that $\mathbf{M}^k = \mathbf{0}$.

If $\mathbf{M}$ is a nilpotent matrix, then the smallest positive integer ν for which $\mathbf{M}^\nu = \mathbf{0}$ and $\mathbf{M}^{\nu-1} \neq \mathbf{0}$ is called the *index of nilpotency*.

The following theorem precedes the definition of the index of a linear constant coefficient DAE.

Theorem 4.1 (Kronecker)**.** *Let $\lambda\mathbf{A}+\mathbf{B}$ be a regular matrix pencil. Then, there exist non-singular matrices $\mathbf{P}$ and $\mathbf{Q}$ such that*

$$\mathbf{PAQ} = \begin{bmatrix} \mathbf{I} & \mathbf{0} \\ \mathbf{0} & \mathbf{N} \end{bmatrix} \qquad \mathbf{PBQ} = \begin{bmatrix} \mathbf{C} & \mathbf{0} \\ \mathbf{0} & \mathbf{I} \end{bmatrix},$$

where $\mathbf{I}$ is an identity matrix and $\mathbf{N}$ a nilpotent matrix of index k.

Definition 4.9 (*Index of a linear coefficient DAE*)**.** Let $\lambda\mathbf{A} + \mathbf{B}$ be a regular matrix pencil, then the index of nilpotency, or index for short, of the linear constant coefficient DAE (4.5) is the index of nilpotency, k, of the matrix $\mathbf{N}$ defined in Theorem 4.1.

If $\mathbf{N} = \mathbf{0}$, then define $k = 1$. In the case of a non-singular matrix $\mathbf{A}$, the index is defined as $k = 0$.

An important consequence of Kronecker's theroem is that the solution of the DAE system 4.5 can be given in analytical form. Suppose that the matrices $\mathbf{P}$ and $\mathbf{Q}$ in Theorem (4.1) are known. Then, by means of the transformation

$$\mathbf{x} = \mathbf{Q} \begin{bmatrix} \mathbf{y}_1 \\ \mathbf{y}_2 \end{bmatrix}$$

and by scaling of Equation 4.5 using the matrix $\mathbf{P}$, the DAE system can be split into two uncoupled subsystems for which the analytical solution is known. With this transformation and the definition

$$\mathbf{Pf}(t) =: \begin{bmatrix} \mathbf{g}_1(t) \\ \mathbf{g}_2(t) \end{bmatrix},$$

an explicit first order ODE for $\mathbf{y}_1$ and a singular subsystem in canonical form for the unknown $\mathbf{y}_2$ results.

$$\dot{\mathbf{y}}_1 \; + \; \mathbf{C}\mathbf{y}_1 = \mathbf{g}_1 \tag{4.6a}$$

$$\mathbf{N}\dot{\mathbf{y}}_2 \; + \; \mathbf{y}_2 = \mathbf{g}_2 \tag{4.6b}$$

Let $\mathscr{L}_-$ denote the Laplace operator

$$(\mathscr{L}_- x)(s) \; := \; \int_{0-}^{\infty} x(\tau) e^{-s\tau} d\tau \; , \tag{4.7}$$

where $s \in \mathbb{C}$ ([21], Section 1.2), then the Laplace transform of Equation 4.6b yields

$$\begin{aligned}(\mathscr{L}_- \mathbf{y}_2)(s) &= (\,\mathbf{N}s + \mathbf{I})^{-1}\mathbf{N}\mathbf{y}_2(0-) \; + \; (\,\mathbf{N}s + \mathbf{I})^{-1}(\mathscr{L}_- \mathbf{g}_2)(s) \\ &= \sum_{i=0}^{\infty} (-1)^i \, (\mathbf{N}s)^i \mathbf{N}\mathbf{y}_2(0-) \; + \\ &\quad \sum_{i=0}^{\infty} (-1)^i \, (\mathbf{N}s)^i (\mathscr{L}_- \mathbf{g}_2)(s) \; . \end{aligned} \tag{4.8}$$

Since $\mathbf{N}$ is a nilpotent matrix of index k, the infinite series reduces to a sum with a finite number of terms. Transformation back into the time domain gives $\mathbf{y}_2(t)$.

$$\mathbf{y}_2(t) \; = \; \sum_{i=0}^{k-1} (-1)^i \, \mathbf{N}^i \, \delta^{(i)} \mathbf{N}\mathbf{y}_2(0-) \; + \; \sum_{i=0}^{k-1} (-1)^i \, \mathbf{N}^i \, \mathbf{g}_2^{(i)}(t) \; , \tag{4.9}$$

where $\delta^{(i)}$ denotes the i^{th} derivative of the Dirac pulse. Apparently, the Dirac pulse and its derivatives vanish and with it a source for big errors in the numerical solution due to a limited machine precision if values $\mathbf{y}_2(0-)$ vanish. If the index of the DAE system is > 1, then the solution of the subsystem (4.6b) includes the derivatives of the function $\mathbf{g}_2$ up to the order $k-1$. Their computation, if numerically performed, is ill conditioned. This problem does not appear if the matrix $\mathbf{A}$ in Equation 4.5 is non-singular. Then, Equation 4.5 is not truly a DAE but an ODE. The solution of the explicit ODE, Equation 4.6a, is

$$\mathbf{y}_1 \; = \; \mathbf{e}^{-\mathbf{C}t}\mathbf{y}_1(0) \; + \; \int_0^t \mathbf{e}^{-\mathbf{C}(t-\tau)} \, \mathbf{g}_1(\tau) d\tau \tag{4.10}$$

for every initial value $\mathbf{y}_1(0)$.

Definition 4.10 (*Local index of a linear time-variant DAE***).** If the coefficient matrices in Equation 4.5 are time dependent, then the *local* index is the index of the DAE system for some time t. It is denoted by $k(t)$.

For general nonlinear implicit differential-algebraic systems

$$\mathbf{F}(\,\dot{\mathbf{y}},\, \mathbf{y}, t\,) \; = \; \mathbf{0} \; , \tag{4.11}$$

a so-called *differential* index has been introduced by Gear [14].

Definition 4.11 (*Differential index of a nonlinear DAE system***).** If the matrix $\partial \mathbf{F}/\partial \dot{\mathbf{y}}$ is non-singular, the index k is set to zero, $k = 0$. (In this case Equation 4.11 is an implicit ODE that, in principle, can be transformed into an explicit ODE.)

Otherwise, the following set of equations is established by repeated differentiation of Equation 4.11 with respect to time

$$\begin{aligned}
\mathbf{0} &= \mathbf{F}(\,\dot{\mathbf{y}},\,\mathbf{y},t\,) \\
\mathbf{0} &= \frac{d}{dt}\mathbf{F} \;=\; \frac{\partial \mathbf{F}}{\partial \dot{\mathbf{y}}}\,\ddot{\mathbf{y}} + \frac{\partial \mathbf{F}}{\partial \mathbf{y}}\,\dot{\mathbf{y}} + \frac{\partial \mathbf{F}}{\partial t} \\
\mathbf{0} &= \frac{d^2}{dt^2}\mathbf{F} \;=\; \frac{\partial \mathbf{F}}{\partial \dot{\mathbf{y}}}\,\mathbf{y}^{(3)} + \dots \\
&\;\;\vdots \\
\mathbf{0} &= \frac{d^j}{dt^j}\mathbf{F} \;=\; \frac{\partial \mathbf{F}}{\partial \dot{\mathbf{y}}}\,\mathbf{y}^{(j+1)} + \dots\,,
\end{aligned}$$

in which $\dot{\mathbf{y}}, \dots, \mathbf{y}^{(j+1)}$ are considered separate independent algebraic variables being functions of the variables $\mathbf{y}$ and t (considered independent). Since $\partial \mathbf{F}/\partial \dot{\mathbf{y}}$ is singular, it is not possible to solve for the highest derivative $\mathbf{y}^{(j+1)}$. However, if it is possible to solve for $\dot{\mathbf{y}}$ for some finite j, then the smallest j, for which this is possible, is defined the differential index k of the differential-algebraic system, Equation 4.11.

Remark 4.5. 1. Repeated differentiation of the initial DAE provides additional equations. If the resulting set of equations is solvable for $\dot{\mathbf{y}}$, the problem of solving the initial DAE can be transformed into the problem of solving an explicit ODE. In the above scheme, all equations of (4.11) are differentiated with respect to time, although it may be sufficient to differentiate only some of them in order to determine $\dot{\mathbf{y}}$ as a continuous function of $\mathbf{y}$ and t. In [14], Gear gives an algorithm by which only equations are differentiated that do not include components of $\dot{\mathbf{y}}$.

2. For linear constant coefficient DAEs (Equation 4.5), the differential index equals the index of nilpotency introduced in Definition 4.9.

If the state vector $\mathbf{x}$ and the vector of algebraic variables $\mathbf{h}$ in the hydraulic bridge example are combined into a vector $\mathbf{y}$, then one step of differentiation yields that the DAE system is of index one if the partial derivative of the algebraic constraint with respect to $\mathbf{y}$ is non-singular (cf. Equations 4.2a, 4.2b or Equations 4.4a, 4.4b).

For DAE systems of the form

$$\mathbf{0} = \mathbf{f}_1(\dot{\mathbf{x}}, \mathbf{x}, \mathbf{z}, t) \tag{4.12a}$$

$$\mathbf{0} = \mathbf{f}_2(\mathbf{x}, \mathbf{z}, t)\;\;, \tag{4.12b}$$

also called *semi-state systems* or *systems in descriptor form*, the definition of the differential index can be reformulated.

Definition 4.12 (*Differential index of a semi-state system***).** The index of a semi-state system is the minimum number of times that the algebraic part (4.12b) must be differentiated with respect to time in order to determine $\dot{\mathbf{x}}$ as a continuous function of the state vector $\mathbf{x}$, the vector of so-called *semi-state variables* $\mathbf{z}$ and time t.

For linear time-variant differential-algebraic systems, Gear and Petzold have given an algorithm on matrices that can be used for the determination of the index [15]. Since in the following we want to determine the local index for some examples, we recall the algorithm for the determination of the index of linear constant coefficient DAEs [8].

Algorithm 4.1 (Index determination for linear constant coefficient DAEs).

1. *The index k is initialised with zero.*
2. *If the matrix $\mathbf{A}$ in Equation 4.5 is non-singular, we are done. No further iteration is necessary. The algorithm terminates.*
3. *Otherwise, Equation 4.5 is pre-multiplied by a non-singular matrix $\mathbf{P}$ that transforms the DAE into the form*

$$\begin{bmatrix} \mathbf{A}_{11} & \mathbf{A}_{12} \\ \mathbf{0} & \mathbf{0} \end{bmatrix} \begin{bmatrix} \dot{\mathbf{x}}_1 \\ \dot{\mathbf{x}}_2 \end{bmatrix} + \begin{bmatrix} \tilde{\mathbf{B}}_{11} & \tilde{\mathbf{B}}_{12} \\ \tilde{\mathbf{B}}_{21} & \tilde{\mathbf{B}}_{22} \end{bmatrix} \begin{bmatrix} \mathbf{x}_1 \\ \mathbf{x}_2 \end{bmatrix} = \begin{bmatrix} \tilde{\mathbf{f}}_1 \\ \tilde{\mathbf{f}}_2 \end{bmatrix} ,$$

   in which the row-rank of the matrix $[\,\mathbf{A}_{11}\ \mathbf{A}_{12}\,]$ equals the number of its rows.
4. *After differentiation of the algebraic equation $\tilde{\mathbf{B}}_{21}\mathbf{x}_1 + \tilde{\mathbf{B}}_{22}\mathbf{x}_2 = \tilde{\mathbf{f}}_2$, we get the new system*

$$\begin{bmatrix} \mathbf{A}_{11} & \mathbf{A}_{12} \\ \tilde{\mathbf{B}}_{21} & \tilde{\mathbf{B}}_{22} \end{bmatrix} \begin{bmatrix} \dot{\mathbf{x}}_1 \\ \dot{\mathbf{x}}_2 \end{bmatrix} + \begin{bmatrix} \tilde{\mathbf{B}}_{11} & \tilde{\mathbf{B}}_{12} \\ \mathbf{0} & \mathbf{0} \end{bmatrix} \begin{bmatrix} \mathbf{x}_1 \\ \mathbf{x}_2 \end{bmatrix} = \begin{bmatrix} \tilde{\mathbf{f}}_1 \\ \dot{\tilde{\mathbf{f}}}_2 \end{bmatrix} .$$

5. *The index is increased by one. The old system is replaced by the new one. The algorithm continues with step 2.*

Remark 4.6. If the algorithm terminates after k iterations, then the DAE system in the last iteration has the index zero. The DAE system in the next to last iteration is of index one. The original DAE system then has the index k. That is, the algorithm not only determines the index. Actually, it does an index reduction.

In general, the algebraic constraints of a DAE system are nonlinear as in the considered example of a hydraulic Wheatstone bridge. Hence, for each time t_n, often, they can be solved only numerically by iteration. If Equations 4.2a–4.2b derived from a bond graph with causal paths between resistive ports are linearised, then the local index of the linearised system equals one [32]. This means that they can be solved by means of an ODE based method. A widely used code for the numerical solution of DAE systems of index < 2 has become the solver called DASSL [8]. Public domain mathematical software such as Scilab [11, 29] or GNU Octave [2] provide a function that calls the DASSL code. In addition, Octave [2] includes a function that calls DASPK [1, 30] a further development of the DASSL code.

4.3 Inserting Energy Stores into Causal Paths Between Resistive Ports

It is certainly an essential objective of object-oriented methodologies to separate the modelling phase from the formulation of equations and their numerical solution in order to achieve consistency in the development of large models. Following an object-oriented approach, the interfaces of submodels are connected according to the topology in a system schematic. Constitutive equations of the submodels are expected to be reformulated automatically, if required by the interconnection of the submodels. If library submodels are protected from modifications by the developer of a system model, then obviously less errors can occur. On the other hand, the model developer cannot affect the generation of system equations. Still, on a lower level, there are relations between decisions taken in the modelling phase and aspects with regard to the numerical solution of the generated equations. In former times, when no solvers for differential-algebraic equations systems were available, these relations were frequently used. Even with today's solvers, it makes sense to take into account aspects of an efficient numerical solution of the generated equations in the phase of the model development. Moreover, it may be useful to have the generated equations undergo a symbolic preprocessing before they are passed on to a numerical solver. For instance, it is well known that problems with the numerical solution of DAEs increase with an increase of their index. In Chapter 5, relations between bond graph modelling and the symbolic and numerical solution of system equations will be considered in detail. In the following, first, simple possibilities will be discussed to affect the form of the resulting mathematical model already in the modelling phase.

The algebraic constraints 4.2a can be avoided by inserting energy stores into causal paths between resistive ports. In order to ensure that the dynamic behaviour of the original model is not perceptibly affected, additional energy stores must be small. In complex nonlinear models, it is not easy to estimate how small parameter values of additional energy stores must be. On the other hand, including small energy stores may be justified from physics. There are always dynamic effects that are often neglected because their impact on the overall dynamic behaviour of the system is assumed to be negligible. In the bond graph of Figure 4.2, the two disjoint causal paths between resistors may be removed by adding two C energy stores to the lower 0-junctions accounting for the oil compliance in the volumes of the cylinder in the load diagonal of the bridge (Figure 4.5). From the modified bond graph in Figure 4.5, a state space model of order 3 may be derived so that a DAE solver is not necessary. As the added C elements are linear, the two additional ODEs can be written in the form

$$C_1\,\dot{p}_{C_1} = g_1(p_1) + A\,v - Q_2 \tag{4.13a}$$

$$C_2\,\dot{p}_{C_2} = g_4(p_4) - A\,v - Q_3\,. \tag{4.13b}$$

For $C_1, C_2 \to 0$, the two ODEs turn into the algebraic Equations 4.1b and 4.1e.

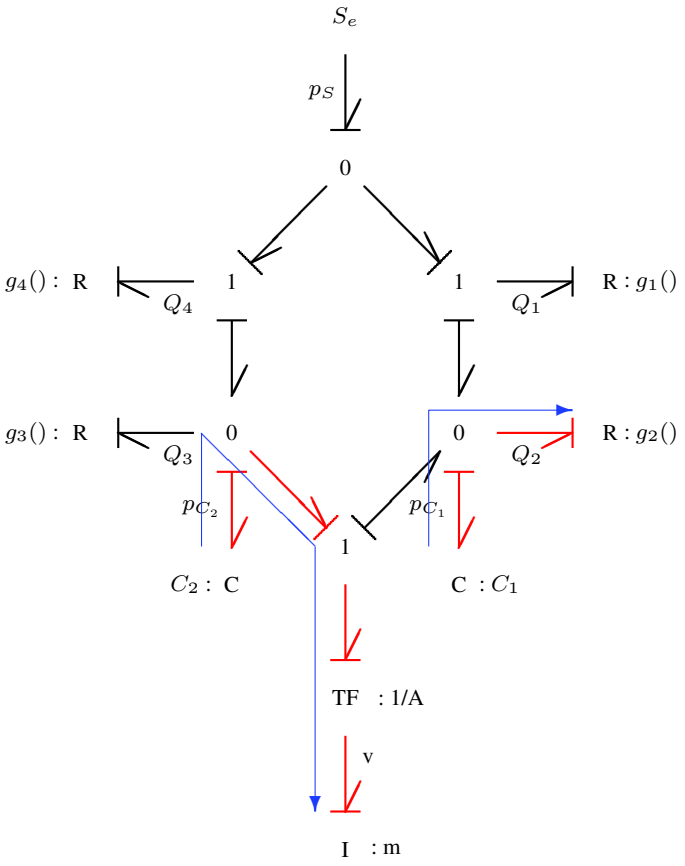

Fig. 4.5 Removal of causal paths between resistors by inserting C energy stores

Disadvantages of such an approach are that the order of the system is increased and that fast dynamic transients are introduced because the capacitances C_1 and C_2 of the added energy C stores are small. Hence, it is true that the result is a set of explicit ODEs, but its solution requires a small step size or an implicit numerical integration algorithm.

Estimation of the Time Constants of a Linear Model

It is well known that if a set of linearised ODEs is solved by means of an explicit numerical integration algorithm, then its step size must be chosen smaller than the smallest time constant. The determination of the time constants means the determination of eigenvalues which is quite costly. A rough estimate, however, can be obtained directly from the bond graph by following causal paths between storage ports and resistive ports. Suppose constitutive equations are linear or have been

linearised, then such causal paths identify first order transients considered isolated from other transients in the system and isolated from forcing inputs.

In Figure 4.5, their time constant is just the product of the parameters of the storage port at one end of the causal path and of the resistive port at its other end. To see this, the following equations are derived from the bond graph in Figure 4.5.

$$Q_2 = g_2\,(p_{C_1}) \tag{4.14a}$$

$$\dot{p}_{C_1} = \frac{1}{C_1}\,[\,Q_1 \,+ A\,v \,-\, Q_2\,] \tag{4.14b}$$

Consider the homogeneous ODE

$$\dot{p}_{C_1} \,+\, \frac{1}{C_1}\,g_2\,(p_{C_2}) \;=\; 0\;. \tag{4.15}$$

If the nonlinear characteristic of g_2 is replaced by a linear one of slope $1/R_2$ in the neighbourhood of an operating point, then the time constant, τ_{12}, of the free response given by Equation 4.15 is $\tau_{12} \;=\; R_2C_1$. Apparently, by considering all causal paths between storage ports and resistive ports, the smallest time constant can be determined. However, it must be kept in mind that transients are considered decoupled this way. This, however, is not true. The evaluation of the exact value of the smallest time constant requires the solution of an eigenvalue problem. The corresponding considerable effort, however, is not worthwhile. Anyway, the usefulness of an estimation of the time constants is limited to systems of linear constant coefficient ODEs that are solved by means of an explicit integration algorithm. The inspection of the bond graph with regard to time constants of isolated transients may give an indication of how widely time constants are separated when small energy stores are included into the bond graph in order to avoid algebraic loops.

In addition to these first order transients, the C energy stores included in the bond graph of Figure 4.5 lead to another oscillations that are identified by causal paths between a C element and the I energy store. In addition to Equation 4.14b, the following state equation is immediately obtained from the bond graph.

$$\dot{v} \;=\; \frac{A}{m}\,(\,p_{C_2} \,-\, p_{C_1}\,) \tag{4.16}$$

By differentiation of Equation 4.14b and substituting it into the state equation of the I energy store, a second order ODE results for the output of the C energy store with capacitance parameter C_1.

$$\ddot{p}_{C_1} \,+\, \frac{1}{C_1}\,\frac{A^2}{m}\,p_{C_1} \;=\; \frac{1}{C_1}\,(\,\dot{Q}_1 \,-\, \dot{Q}_2 \,+\, \frac{A^2}{m}\,p_{C_2}\,) \tag{4.17}$$

The natural frequency of the free undamped oscillation of pressure p_{C_1} reads

$$\omega_0^2 = \frac{A^2}{C_1\,m}\;. \tag{4.18}$$

For small values of the fluid filled volume V_1 or the mass m, C energy stores for the fluid compliance in the volumes V_1 and V_2 can remove causal paths between resistive ports, but introduce high frequent oscillations superimposed on the dynamics of the pressures in the volumes. They may be damped by attaching resistors with a small parameter to the 0-junctions representing the two pressures p_{C_1} and p_{C_2}. However, in the case of an explicit integration algorithm, a small step size is still required.

These considerations show that in the case of causal paths between resistive ports, a DAE system can be avoided by including energy stores with a small parameter. Solution of the resulting ODE system, however, generally requires a stiffly stable integration algorithm. Of course, the ODE system derived from the modified bond graph can be converted into a DAE system. If capacitances tended to zero, the ODEs of the C energy stores reduce to algebraic constraints for the pressures in the volumes of the cylinder.

Finally, particularities of a model, if there are any, can be used to remove causal paths between resistive ports. If, for instance, the resistors of a bridge circuit are the control orifices of a spool valve with zero overlap in the central position, then two orifices in a diagonal are always open while the other two are closed. This can be used for a model reduction that removes the causal paths between resistive ports. Although such an approach leads to a model allowing for an efficient numerical computation, it is not generally applicable. On the other hand, it is always possible to include energy stores with small parameters. However, it appears that there is only a need for modifying a model this way if the available modelling and simulation software does not accept DAEs of index one and if a model reduction is not possible.

4.4 Causal Paths Between Storage Ports of the Same Type

In this section, we will exclude causal paths between resistive ports. Instead, we will consider causal paths between independent and dependent storage ports (van Dijk calls them *class-1 zero-order causal paths* [32]). Such causal paths often appear in bond graphs of multibody systems with algebraic contraints between the velocities of some rigid bodies caused by joints connecting them. In Section 3.4, we already considered a simple example of two inertias coupled by a transformer with constant modulus (Figure 3.14). In this case, the dependent energy store can be transformed over the transformer and can be combined with the independent one into a new one with integral causality. If energy stores have a linear characteristic, then C energy stores attached to a 0-junction or I energy stores connected to a 1-junction can be combined into one equivalent energy store.

If such reductions are not possible or if they are not performed, then the mathematical model to be derived from a bond graph with causal paths between storage ports of the same type is of the form of a DAE system

$$\dot{\mathbf{x}}_i(t) = \mathbf{f}_1\,(\,\mathbf{x}_i(t), \dot{\mathbf{x}}_d(t),\, \mathbf{u}(t)\,) \tag{4.19a}$$

$$\mathbf{x}_d(t) = \mathbf{f}_2\,(\,\mathbf{x}_i(t), \mathbf{u}(t)\,)\;. \tag{4.19b}$$

In Equations 4.19a and 4.19b, $\mathbf{x}_i$ denotes the vector of independent state variables, whereas $\mathbf{x}_d$ is the vector of dependent state variables. Again, $\mathbf{u}$ is the vector of all system inputs.

Van Dijk has shown that the linearised DAE system obtained from a bond graph with causal paths between independent and dependent storage ports is of local index one [32].

Example: Slider Crank Mechanism

For illustration, consider the often used example of a simple slider crank mechanism depicted in Figure 4.6. A *massless* rod of length L links a flywheel of moment of inertia J to a piston of mass m. In [3], Allen considers a similar slider crank mechanism as an introductory example in the context of establishing Lagrange's equations for complex mechanical mechanism (cf. Section 4.10).

The rod establishes a geometric constraint between the angular position, $\varphi(t) := \int_0^t \omega(\tau)d\tau$, of the flywheel and the position of the piston. Differentiation with respect to time yields a constraint between the angular velocity, ω, and the translational velocity, v, of the piston

$$v \;=\; T(\varphi) \times \omega \tag{4.20}$$

and

$$T(\varphi) \;=\; \frac{r\,(\,r\cos\varphi \;+\; \sqrt{L^2 \;-\; r^2\,\sin^2\varphi}\,)\,sin\varphi}{\sqrt{L^2 \;-\; r^2\,\sin^2\varphi}}\;. \tag{4.21}$$

Assuming that rotational power is transformed into translational power without any losses, yields for the moment $\tilde{M}$ transformed into the force $\tilde{F}$ acting on the piston

$$\tilde{M} \;=\; T(\varphi)\,\tilde{F}\;. \tag{4.22}$$

Thus, this transformation can be represented by a displacement modulated transformer of modulus $T(\varphi)$. Such transformers are often used for representing trans-

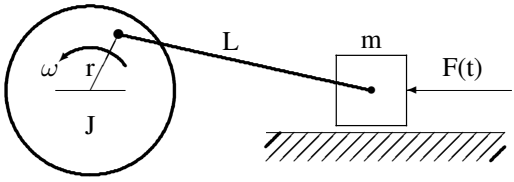

Fig. 4.6 Slider crank mechanism

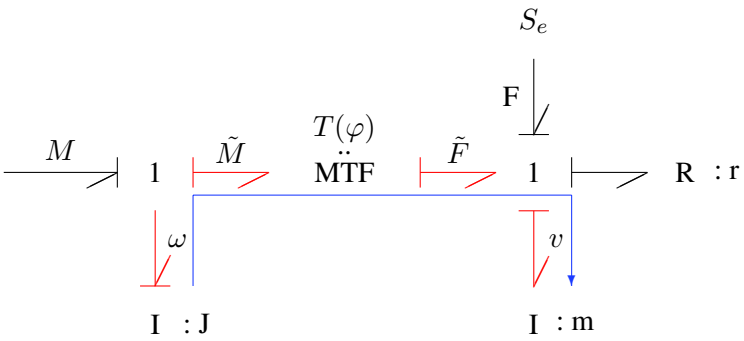

Fig. 4.7 Bond graph of the slider crank mechanism

formations between reference frames when the planar or 3D motion of mechanical systems is modelled. They have no counterpart in electrical engineering. Due to the constraint of the velocities, one I element in the bond graph of Figure 4.7 must have derivative causality. For the energy store with preferred integral causality, the state equation

$$\dot{\omega} = \frac{1}{J}\left[M - T(\varphi) \times \left(m\,\dot{v} + r\,v - F\right)\right] \tag{4.23}$$

is derived from the bond graph. In addition to the angular velocity ω in this example, the kinematic displacement of the φ is needed as another state variable which is typical for modelling planar or 3D motion of mechanical systems.

$$\dot{\varphi} = \omega \tag{4.24}$$

All three equations can be combined into a linear implicit DAE system also called a linearised descriptor form [13, 24].

$$\begin{bmatrix} J & T\,m & 0 \\ 0 & 0 & 1 \\ 0 & 0 & 0 \end{bmatrix} \begin{bmatrix} \dot{\omega} \\ \dot{v} \\ \dot{\varphi} \end{bmatrix} + \begin{bmatrix} 0 & Tr & 0 \\ -1 & 0 & 0 \\ T & -1 & 0 \end{bmatrix} \begin{bmatrix} \omega \\ v \\ \varphi \end{bmatrix} = \begin{bmatrix} M + T\,F \\ 0 \\ 0 \end{bmatrix} \tag{4.25}$$

Due to the algebraic dependency between the velocities, the matrix pre-multiplying the time-rate of the descriptor vector is singular. Thus, the mathematical model derived from a bond graph with a causal path between an independent and a dependent storage port, in fact, takes the form of a true DAE system. If algorithm 4.1 is applied to this DAE, then the matrix pre-multiplying the time-rate of the descriptor vector becomes non-singular after one step. Hence, the local index of the DAE system equals one as to be expected.

The DAE system can be avoided, i.e., an explicit state space model can be derived, if the dependent energy store is transformed over the transformer like in the example of Figure 3.14. However in contrast to that example, here, the modulus of the transformer is not constant. Hence, the inertia of the resulting I element is not

constant. We come back to this issue in Section 4.10 when we consider the derivation of Lagrange's equations from bond graphs. Another option that can be justified from physics is to neutralise the kinematic constraint by assuming that the rod is not completely rigid, but has some compliance. With this assumption, a C energy store with a small parameter can be used to remove the causal path between the two inertias. Like in the hydraulic bridge example (Figure 4.2), this leads to a high frequency oscillation that can be damped by including a resistor in addition to the C energy store. The resistor may also be justified for physical reasons. Taking a closer look at the rod, it turns out that it is not a purely elastic, but quite stiff link. There are also energy losses in the rod. The simplest approximation to a continuum model is to use a pair of C and R elements along with parameters that are estimated on the basis of experience. For numerical stability, it is reasonable to use an implicit integration algorithm.

4.5 Closed Causal Paths

So far, causal paths between resistive ports or between independent and dependent storage ports have been considered. In addition, closed causal paths in the junction structure can occur. They are called *causal loops* (Definition 3.10).

For illustration, consider the simple example of a bond graph with a bond loop displayed in Figure 4.8. Figure 4.9 shows an electrical circuit that can be represented by the bond graph in Figure 4.8. As can be seen from the bond graph of Figure 4.8, the causality of the flow source and the preferred integral causality of the energy stores do not propagate into the junction structure. In this simple example, there is a need to perform step 5 of the sequential causality assignment procedure by choosing a bond and assigning causality to it. This gives rise to the introduction of the notion of *strong* (*weak*) causal determination.

Definition 4.13 (*Strong (weak) causal determination of a junction***).** A bond imposes a *strong* causal determination on a junction J it is connected to if one of its power conjugate variables determines the variable common to all remaining adjacent bonds. Otherwise, the bond gives a *weak* causal determination to the junction [26].

Remark 4.7. If the causal stroke of a bond connected to a 0-junction is on its end attached to the 0-junction, then the effort common on all adjacent bonds is determined. That is, the effort imposed on a 0-junction is propagated to ports connected to it.

In the example of Figure 4.8, the two 0-junctions have a *weak* causal determination. In order to complete causality assignment, causality must be chosen at one internal bond (Definition 2.9) No matter which bond is chosen, the result is a causal loop (Definition 4.6) associated with two open signal flow loops of opposite orientation as depicted in Figure 4.10. One signal flow loop only relates the efforts of the

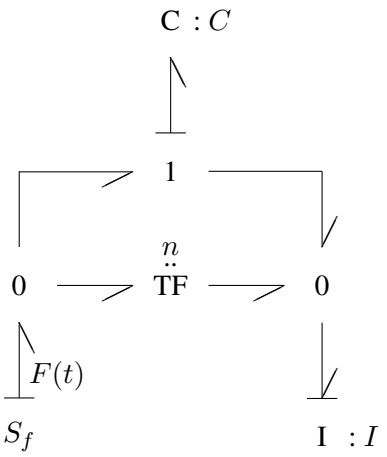

Fig. 4.8 Bond graph with a bond loop

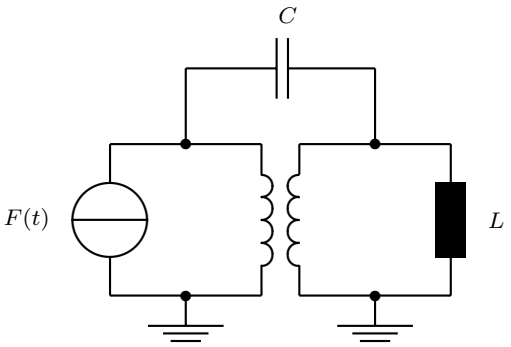

Fig. 4.9 Circuit realisation of the bond graph with a bond loop

internal bonds, while in the other, only the corresponding flows are involved. Thus, each algebraic loop contributes an auxiliary variable. If the outputs of the transformer e_4 and f_3 are chosen as auxiliary variables, then the following equations can be derived from the bond graph of Figure 4.10

$$0 = e_4 - \frac{1}{n} e_4 - e_C \tag{4.26a}$$

$$0 = F - \frac{1}{n} f_3 + f_3 - f_I \tag{4.26b}$$

$$\dot{e}_C = \frac{1}{C} \left(F - \frac{1}{n} f_3 \right) \tag{4.26c}$$

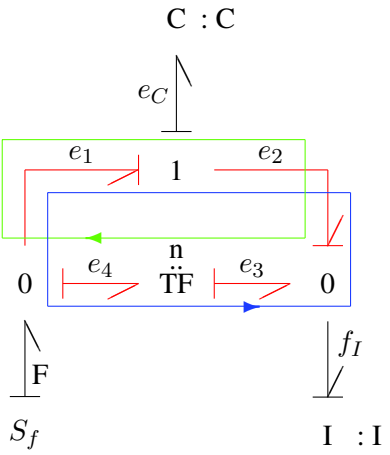

Fig. 4.10 Bond graph with causal loop and two associated topological loops

$$\dot{f}_I = \frac{1}{I}\,(\,e_4 - e_C\,)\,. \tag{4.26d}$$

Since in this example the system of equations determining the algebraic variables is linear, it can be symbolically solved and the algebraic variables can be removed from the state equations.

$$\dot{e}_C = \frac{1}{C(n-1)}\,[\,nF - f_I\,] \tag{4.27a}$$

$$\dot{f}_I = \frac{1}{I(n-1)}\,e_C \tag{4.27b}$$

However, as can be seen from the result, this elimination step is only possible for a transformer modulus $n \neq 1$. Ort and Martens [26] have given a mathematical criterion for the solvability of the algebraic equations of the junction structure. In [28], Rosenberg and Andry have given a criterion that can be directly checked on the bond graph. First, consider the mathematical criterion applied to our example. By looking at the bond graph in Figure 4.10, the following equations for efforts can be written.

$$\left[\begin{array}{c} e_S \\ e_I \\ \hline e_1 \\ e_2 \\ e_3 \\ e_4 \end{array}\right] = \left[\begin{array}{c|cccc} 0 & 0 & 0 & 0 & 1 \\ 0 & 0 & 1 & 0 & 0 \\ \hline 0 & 0 & 0 & 0 & 1 \\ -1 & 1 & 0 & 0 & 0 \\ 0 & 0 & 1 & 0 & 0 \\ 0 & 0 & 0 & n & 0 \end{array}\right] \left[\begin{array}{c} e_C \\ \hline e_1 \\ e_2 \\ e_3 \\ e_4 \end{array}\right] \tag{4.28}$$

Let us combine the efforts that are outputs of the junction structure into a vector $\mathbf{e}_{out} = (e_S, e_I)^T$ and all internal efforts into a vector $\mathbf{e}_{int} = (e_1, e_2, e_3, e_4)^T$.

The vector of efforts that are input to the junction structure has only one component $\mathbf{e}_{in} = (e_C)$. With these vectors, the system of equations 4.28 has the form

$$\begin{bmatrix} \mathbf{e}_{out} \\ \mathbf{e}_{int} \end{bmatrix} = \begin{bmatrix} \mathbf{S}_1 & \mathbf{S}_2 \\ \mathbf{S}_3 & \mathbf{S}_4 \end{bmatrix} \begin{bmatrix} \mathbf{e}_{in} \\ \mathbf{e}_{int} \end{bmatrix} . \tag{4.29}$$

In general, the system of equations 4.29 can be solved for $\mathbf{e}_{int}$ if $\det(\mathbf{I} - \mathbf{S}_4) \neq 0$. The dimension of the identity matrix $\mathbf{I}$ equals the number of internal bonds. In the example under consideration, the determinant is equal to $1 - n$. Solvability of the junction structure equations means that the mathematical model can be written in state space form.

Instead of establishing a linear system of junction structure equations and to check for its solvability at the level of equations, it appears to be more convenient to use a criterion that can be directly checked on the bond graph. Such a criterion has been given by Rosenberg and Andry [28]. In order to recall it here, some definitions are needed.

Definition 4.14 (*Influence coefficient*)**.** The influence coefficient of a junction structure node is the ratio of the output variable to the input variable for a particular signal flow loop fragment associated with *two* adjacent bonds of opposite causal orientation [28].

For illustration of this definition, consider the bond graph fragment depicted in Figure 4.11. The causal path $1 - 2 - 3$ is associated with two signal flow loop fragments, one for the efforts of the bonds and one of opposite orientation for the flow variables. Consider the flow variables. They are equal at the 1-junction. Consequently, the influence coefficient $c_{12} = f_1/f_2$ is equal one. The influence coefficient $c_{23} = f_2/f_3$ of the transformer has the value n. Since 1-junctions add up effort variables, the sign of the influence coefficient $c_{21} = e_2/e_1$ depends on the power orientation of the bonds. For the transformer, we have $c_{32} = e_3/e_2 = c_{23}$ (Note that there is another causal path $4 - 2 - 3$).

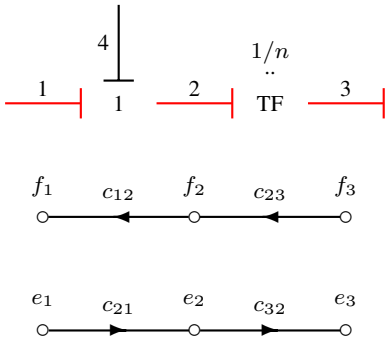

Fig. 4.11 Causal path $1 - 2 - 3$ and associated signal flow loop fragments

Definition 4.15 (*Loop gain of a topological loop***).** The loop gain of a topological loop is the product of all influence coefficients [28].

There are two topological loops of opposite orientation associated with a causal loop in a bond graph (cf. Figure 4.10). It has been shown that the loop gain of both topological loops associated with a causal loop are equal. Hence, due to this unique value, the gain of a causal loop can be defined.

Definition 4.16 (*Causal loop gain***).** The gain of a causal loop is the loop gain of the two topological loops of opposite orientation associated to the causal loop.

The bond graph based rule given by Rosenberg and Andry now states that the linear equations of a general junction structure (GJS) are solvable if and only if causal loops are pairwise disjoint and if the loop gain of every causal loop is different from $+1$. ([28], Theorem 3)

Van Dijk divides causal loops into two classes according to their loop gain. He calls causal loops of loop gain different from one *class-4 zero-order causal paths* and denotes loops of loop gain equal to one as *class-5 zero-order causal paths*. Concerning the local index of a DAE system derived from a bond graph with causal loops, he proves that it is equal to one if, as required in Rosenberg and Andry's theorem, causal loops in the graph are pairwise disjoint and if the loop gain of every causal loop is different from $+1$ ([32], Proposition 5.7).

Let us apply Rosenberg's and Andry's criterion to the example in Figure 4.10. If G_e denotes the loop gain of the topological loop of efforts variables and G_f the loop gain of the signal flow loop of flow variables, then their common value is equal to that of the transformer modulus n.

$$\begin{aligned} G_e &= c_{21} \times c_{32} \times c_{43} \times c_{14} \\ &= 1 \times 1 \times n \times 1 \qquad (4.30a) \\ G_f &= c_{12} \times c_{41} \times c_{34} \times c_{23} \\ &= 1 \times (-1) \times n \times (-1) \qquad (4.30b) \end{aligned}$$

If $n \neq 1$, then the linear equations of the junction structure are solvable, as we know from the previous analysis at equations level.

If the modulus of transformers or the ratio of gyrators is not constant, e.g., there are displacement modulated transformers in the weighted junction structure, then the rule of Rosenberg and Andry is no longer applicable. In that case, the mathematical model takes the form of the Equations 4.2a–4.2b of a DAE system.

Remark 4.8. Since both topological loops associated with a causal loop either relate efforts or flow variables of all bonds of the causal loop, they are open loops according to Definition 4.6. In the bond graph of Figure 4.10, an even number of bonds of the causal loop has the same power orientation. Therefore, its loop gain is positive. If we changed the power orientation of the bond annotated with e_2, then the loop gain would be $(-n)$. In the case of a causal mesh, viz., a closed causal path with an odd number of gyrators (Definition 3.11) , there are also two open loops. The

absolute value of their loop gains is the same. However, they are different in sign. Brown calls a mesh *even* if the loop gain of both open loops of opposite orientation is positive, an *odd mesh* if the loop gain of both open loops is negative, and a *neutral mesh* if the loop gain of both open loops have opposite signs [10]. This way, the Definition 3.9 of a simple even (odd) mesh is extended to general meshes with transformers or gyrators.

4.6 Bond Graphs with Causal Paths from Different Classes

In the previous sections, bond graphs with causal paths from one class only have been considered. Now, bond graphs will be allowed to have causal paths from different classes. We already know that the underlying mathematical model has the form of a DAE system. The interesting question, however, is of what index they are. In the following, we will confine ourselves by considering some examples. A more comprehensive analysis has been performed by van Dijk in [32].

Figure 4.12 shows a modification of the circuit example of Figure 4.9. Consider the associated bond graph displayed in Figure 4.13. There is a causal path $5-2-6-7-8$ between resistors $R_1 - R_2$ and another causal path $1-2-3-4$ between the independent C energy store C_1 and the dependent C energy store C_2. Both causal paths have bond 2 in common. These causal paths result in the following manner. First, causality of the flow source and preferred integral causality at the C energy stores do not propagate into the junction structure. Making a choice and assigning resistance causality to either R_1 or R_2 leads to a causal conflict at the upper 1-junction that can be removed by changing preferred integral causality at C_2 into derivative causality. The result is a causal path between the two energy stores. Assigning conductance causality to either one resistor or to both of them still leaves the bond graph causally incomplete such that causality at one of the bonds of the bond loop must be chosen. The result would be a causal loop. For both open loops associated with this causal loop, two algebraic variables would be needed.

By working along causal paths in the bond graph of Figure 4.13, the following equations can be derived.

$$e_5 = R_1\,[\,n\,(\,F\,-\,f_8\,-\,C_2\,\dot{e}_4)\,+\,C_2\,\dot{e}_4\,] \tag{4.31a}$$

$$f_8 = \frac{1}{R_2}\,n\,(\,e_1\,+\,e_5\,) \tag{4.31b}$$

$$e_4 = (n-1)\,(\,e_1\,+\,e_5\,) \tag{4.31c}$$

$$\dot{e}_1 = \frac{1}{C_1}\,[\,n\,(F\,-\,f_8)\,-\,(n-1)\,C_2\,\dot{e}_4\,] \tag{4.31d}$$

They can be written in the linear implicit form

$$\begin{bmatrix} \mathbf{A}_1 & \mathbf{A}_2 \\ \mathbf{0} & \mathbf{0} \end{bmatrix} \dot{\mathbf{x}} \,+\, \begin{bmatrix} \mathbf{B}_1 & \mathbf{B}_2 \\ \mathbf{B}_3 & \mathbf{B}_4 \end{bmatrix} \mathbf{x} \,=\, \mathbf{b}\,, \tag{4.32}$$

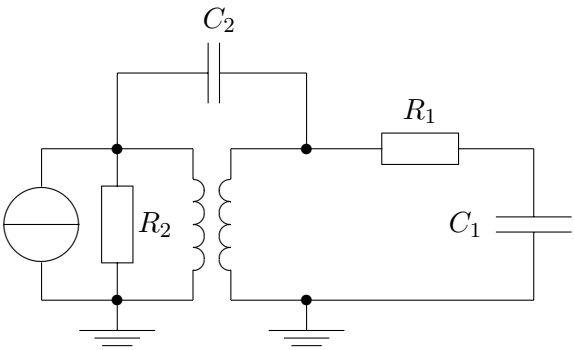

Fig. 4.12 Circuit example

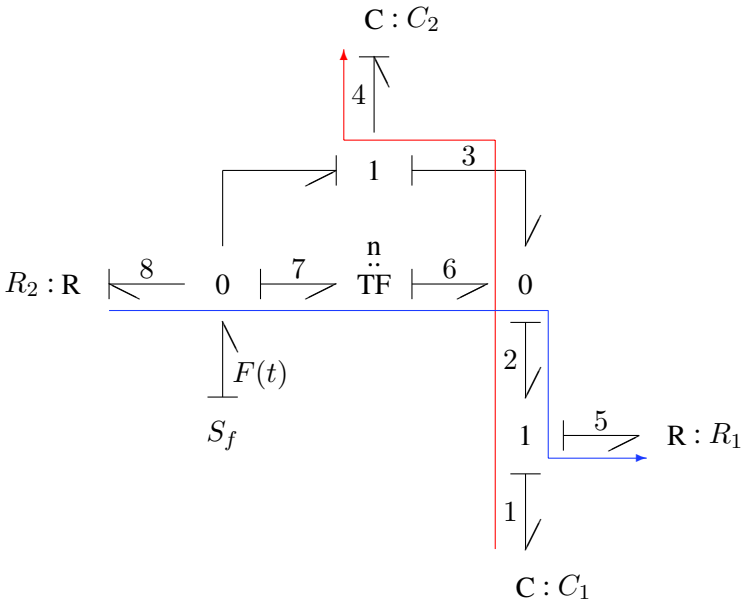

Fig. 4.13 Bond graph with class-2 and class-1 zero-order causal paths

in which the matrix pre-multiplying the derivative of the descriptor vector is singular. Application of algorithm 4.1 yields that the matrix

$$\begin{bmatrix} \mathbf{A}_1 & \mathbf{A}_2 \\ \mathbf{B}_3 & \mathbf{B}_4 \end{bmatrix}$$

is non-singular. That is, the (local) index of the DAE system is equal to one. This result generally holds for bond graphs with causal paths between resistive ports

as well as for bond graphs with causal paths between independent and dependent storage ports [32].

Now, let us modify the bond graph in Figure 4.13 such that in addition to the class 1 zero-order causal path between storage ports, a causal loop results (Figure 4.14). Again, assigning fixed causality to the flow source and integral causality to the energy stores leaves the bond graph causally incomplete. Choosing causality at bond 7 (as depicted in Figure 4.14) leads to a causal conflict at the lower 1-junction that can be removed by changing integral causality at the lower C energy store C_2 into derivative causality. Thus, there are two causal paths, $1-2-3-4-5$ and $1-2-6-7-9$ between both C energy stores. Only one of them has been highlighted for clarity.

Due to the causal loop $6-7-8-2$, the output variables, e_7 and f_6, of the transformer are chosen as auxiliary algebraic variables. Then, the following equations can be written.

$$\dot{e}_1 = \frac{1}{C_1}\left[-f_6 + n_2\, C_2 \cdot \dot{e}_2 + f_{10}\right] \tag{4.33a}$$

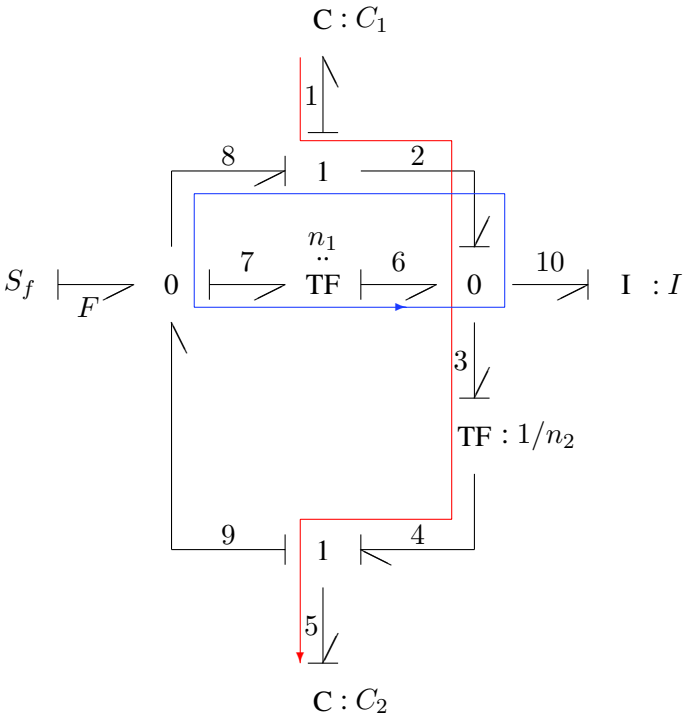

Fig. 4.14 Bond graph with causal loop and class 1 zero-order causal path

$$\dot{f}_{10} = \frac{1}{I}\left[\, e_7 \,-\, e_1 \,\right] \tag{4.33b}$$

$$e_5 = n_2\,(e_7 \,-\, e_1) \,-\, e_7 \tag{4.33c}$$

$$f_6 = n_1\left[\, F \,+\, C_2\,\dot{e}_5 \,-\, (f_{10} \,+\, n_2\,C_2\,\dot{e}_5 \,-\, f_6)\,\right] \tag{4.33d}$$

$$e_7 = n_1\,(\, e_7 \,-\, e_1\,) \tag{4.33e}$$

If they are written in linear implicit form (cf. Equation 4.32), then the matrix premultiplying the descriptor vector is singular, as to be expected. After one step of algorithm 4.1 the resulting matrix

$$\begin{bmatrix} \mathbf{A}_1 & \mathbf{A}_2 \\ \mathbf{B}_3 & \mathbf{B}_4 \end{bmatrix} = \begin{bmatrix} C_1 & 0 & 0 & 0 & -n_2\,C_2 \\ 0 & I & 0 & 0 & 0 \\ 0 & 0 & 0 & 0 & -n_1\,(1-n_2)\,C_2 \\ n_1 & 0 & 0 & (1-n_1) & 0 \\ n_2 & 0 & 0 & (1-n_2) & 1 \end{bmatrix} \tag{4.34}$$

is still singular. Hence, the (local) index is > 1. This result does not hold only for the example for which the index is equal to 2. It can be shown that in general, the local index is > 1, if the bond graph includes class 1 zero-order causal paths that join bonds with causal loops ([32], Proposition 5.10).

4.7 Causal Loops of Unity Loop Gain

Finally, we will address the case of causal loops of unity loop gain by considering the example of the electrical circuit depicted in Figure 4.15 [9, 32]. It will be shown that bond graphs do not directly display Kirchhoff's generalised non-local current law for cut-sets, but indirectly via a causal loop of unity loop gain or by means of a causal conflict at a 0-junction. It appears that the standard sequential causality assignment procedure (SCAP) yields a causal pattern that does not adequately reflect the global continuity of flow variables. This is why van Dijk has proposed a modification of the SCAP that avoids causal loops of unity loop gain. For details, see [32]. Moreover, by means of the delta circuit example (Figure 4.15), we will show that causal loops of unity loop gain can result in DAEs of index > 1. Thus, with regard to a robust numerical solution of the DAE system, they should be avoided.

First, we assume that all passive elements of the delta circuit in Figure 4.15 have an invertible characteristic such that the computational causality at the ports of their corresponding bond graph elements is indifferent. As can be seen from the bond graph in Figure 4.16, fixed causality of the flow source and preferred integral causality at the I energy stores do not propagate into the junction structure.

If conductance causality is chosen at one of the resistor ports, then it imposes a strong causal determination at the 1-junction the resistor is connected to (cf. Definition 4.13). In the end, it results in a causal conflict at a 0-junction (Figure 4.17).

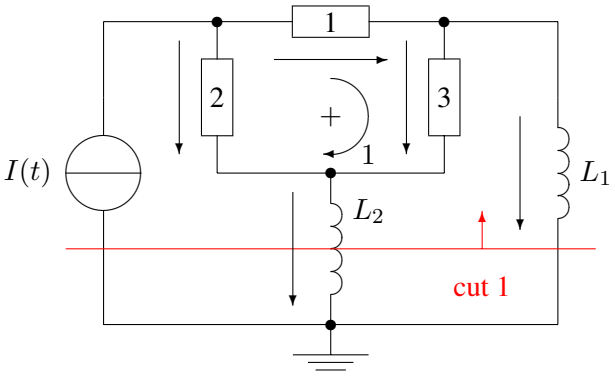

Fig. 4.15 Electrical network with a delta subnetwork of resistors

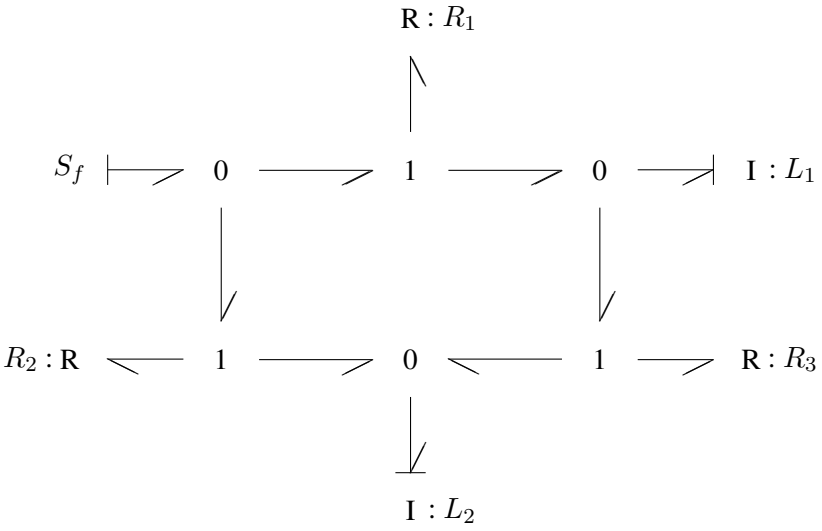

Fig. 4.16 Bond graph of the electrical network

If resistance causality is chosen at the resistive ports in order to avoid a causal conflict, then this causality is not propagated and the bond graph remains causally incomplete. Therefore, causality must be chosen at an internal bond leading to a causal loop. Since there are no transformers or gyrators in the loop, its loop gain is equal to one. There are two open loops of opposite orientation associated to the causal loop as depicted in Figure 4.18.

Consequently, in addition to the outputs of the energy stores, an effort variable must be chosen from one open loop and a flow variable from the other. These have been marked in the bond graph of Figure 4.18. Using these algebraic auxiliary variables, u and i, the following equations can be written

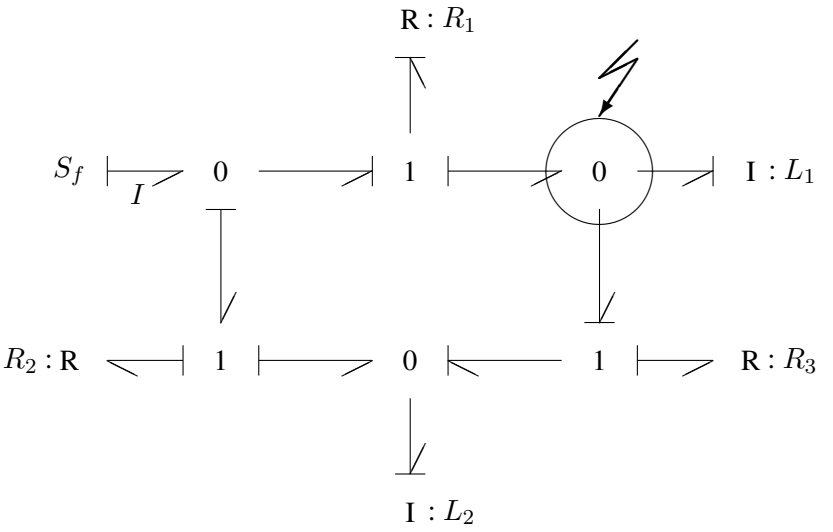

Fig. 4.17 Bond graph with a causal conflict at a 0-junction

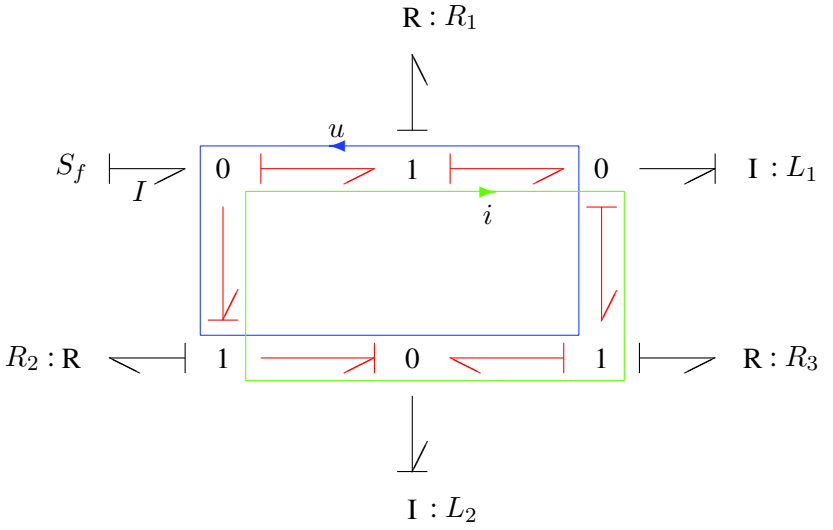

Fig. 4.18 Causal loop with unity loop gain

$$u_1 = R_1\, i \tag{4.35a}$$
$$u_2 = R_2\,(\, I(t) \,-\, i\,) \tag{4.35b}$$
$$u_3 = R_3\,(\, i \,-\, i_{L_1}\,) \tag{4.35c}$$
$$\frac{d}{dt} i_{L_1} = \frac{1}{L_1}\,(\, u \,-\, u_2 \,+\, u_3) \tag{4.35d}$$
$$\frac{d}{dt} i_{L_2} = \frac{1}{L_2}\,(\, u \,-\, u_2\,)\,. \tag{4.35e}$$

Walking along the open loop for the efforts yields

$$u \;=\; u_1 \,+\, u_3 \,+\, u \,-\, u_2\;, \tag{4.36}$$

which is the sum of all voltages around mesh 1 in the circuit (cf. Figure 4.15). From the second topological loop, we obtain Kirchhoff's generalised current law for cut-set 1.

$$i \;=\; I(t) \,-\, i_{L_1} \,-\, i_{L_2} \,+\, i \tag{4.37}$$

The algebraic relation between the outputs of the I energy stores,

$$0 \;=\; I(t) \,-\, i_{L_1} \,-\, i_{L_2}\;, \tag{4.38}$$

can also be obtained from the sum of all flows at the 0-junction with an undetermined common effort if the outputs of the resistors R_1 and R_2 are substituted.

From Equation 4.38, it can be concluded that the delta circuit of the three resistors behaves like a node for which Kirchhoff's current law must hold. In contrast to an actual node, however, it transforms electrical energy into heat. If, in addition to the principle of power conservation, a subsystem complies globally with Kirchhoff's node law, it is said to have the *nodicity* property [19, 33]. The term goes back to Paynter. Electrical networks of passive elements have this nodicity property. In particular for the delta sub-structure of the resistors, continuity of the currents into the structure holds. If the delta structure of resistors is represented by a 3-port, then, according to the causality pattern required for a 0-junction locally representing a balance of flows, an effort should be imposed at one of its ports (Figure 4.19). However, the nodicity property is not directly expressed in the bond graph of Figure 4.18. On the contrary, preferred integral causality at the I energy stores suggests that the currents into the delta subnetwork of resistors are independent. However, due to Kirchhoff's generalised current law for cut-sets (Equation 4.38), this is not true. If according to Equation 4.38, derivative causality is assigned to one of the two I energy stores, say L_1, then the causal loop of unity loop gain disappears. Instead, a causal path $8-9-6-10$ emerges between the energy stores and two other causal paths $1-2-3-4$ and $5-6-7-4$ between resistors $R_3 \,-\, R_1$, or $R_2 \,-\, R_1$ (Figure 4.20).

From the previous section, we know that the DAE system derived from the bond graph in Figure 4.20 is of index one. Hence, it can be numerically solved with a BDF based solver. However, if we leave the causal loop of unity loop gain in the bond graph of Figure 4.18, then the corresponding DAE system is of index > 1. In fact, if

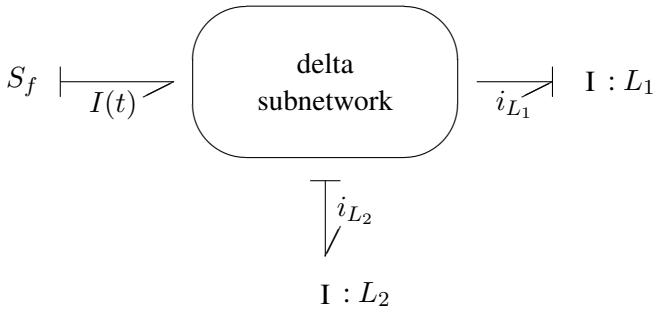

Fig. 4.19 Bond graph of the electrical network using a *nodic* 3-port

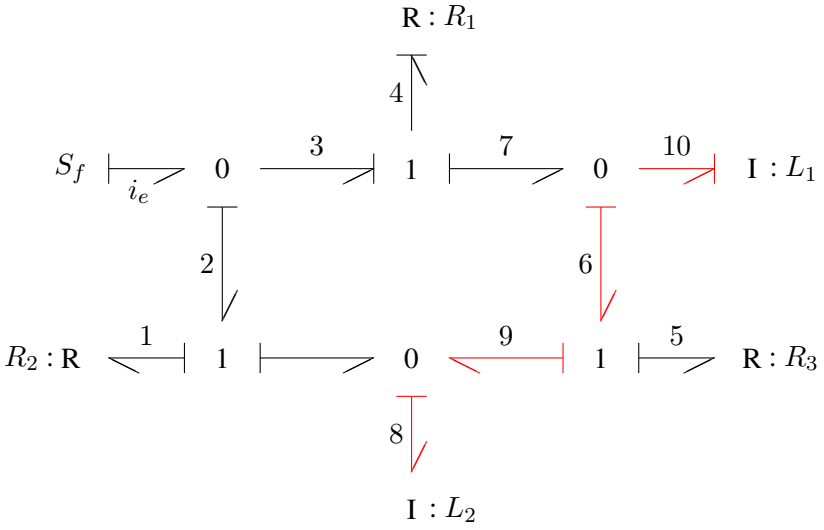

Fig. 4.20 Causalities according to the nodicity property

we write Equations 4.35a–4.35e and Equations 4.36 and 4.38 in linear implicit form

$$\left[\begin{array}{cc|cc} L_1 & 0 & 0 & 0 \\ 0 & L_2 & 0 & 0 \\ \hline 0 & 0 & 0 & 0 \\ 0 & 0 & 0 & 0 \end{array}\right] \frac{d}{dt} \left[\begin{array}{c} i_{L_1} \\ i_{L_2} \\ \hline u \\ i \end{array}\right] + \left[\begin{array}{cc|cc} R_3 & 0 & -1 & -(R_2+R_3) \\ 0 & 0 & -1 & -R_2 \\ \hline -R_3 & 0 & 0 & R_1+R_2+R_3 \\ 1 & 1 & 0 & 0 \end{array}\right] \left[\begin{array}{c} i_{L_1} \\ i_{L_2} \\ \hline u \\ i \end{array}\right] = \left[\begin{array}{c} -R_2 I(t) \\ -R_2 I(t) \\ \hline R_2 I(t) \\ I(t) \end{array}\right], \tag{4.39}$$

then after one step of algorithm 4.1, the resulting matrix

$$\left[\begin{array}{cc|cc} L_1 & 0 & 0 & 0 \\ 0 & L_2 & 0 & 0 \\ \hline -R_3 & 0 & 0 & R_1+R_2+R_3 \\ 1 & 1 & 0 & 0 \end{array}\right]$$

is still singular. Hence, the DAE system is of index > 1.

The problem with the standard sequential causality assignment procedure is that it does not give advice on how to proceed such that the nodicity property is directly expressed in terms of causalities. This was one reason for van Dijk to propose a modification of the SCAP [32].

4.8 Algebraic Loops due to Internal Modulation

From the previous considerations, we know that causal paths between resistive ports, or between independent and dependent storage ports, or closed causal paths in the junction structure represent algebraic constraints such that the mathematical model derived from the bond graph has the form of a DAE system. However, even in bond graphs with no such causal paths, algebraic loops (Definition 4.3) can appear due to so-called *internal modulation*.

Definition 4.17 (*Internal modulation***).** If a bond graph element is modulated by a power variable, then it is said to be *internally modulated*.

For illustration, consider the two examples in Figure 4.21. One constitutive equation of the transformer in Figure 4.21a) reads

$$f_2 \;=\; g\,(f_2)\,f_1\;, \tag{4.40}$$

which cannot be symbolically solved for f_2 in general. Thus, a state equation without algebraic constraint is not possible, although there is no causal path between resistive ports or between independent and dependent storage ports.

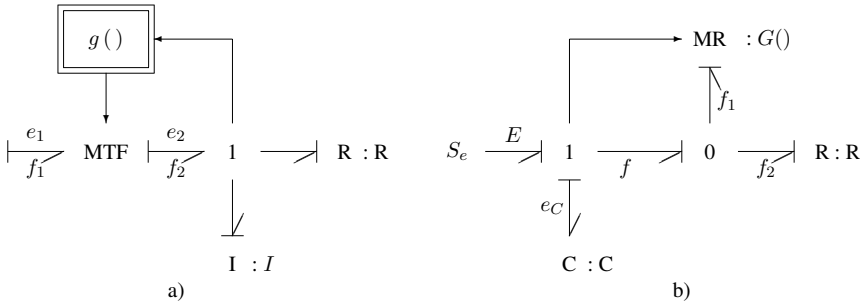

Fig. 4.21 Examples of internal modulation

For the example with the modulated resistor (Figure 4.21b, see also [12]), the following equations can be written

$$f_1 = G\,(\,E - e_C, f_1 + f_2\,) \tag{4.41a}$$
$$f_2 = R\,(E - e_C) \tag{4.41b}$$
$$\dot{e}_C = \frac{1}{C}\,(\,f_1 \,+\, f_2\,)\,. \tag{4.41c}$$

In both cases, modulation by a power variable originating from a junction results in an implicit nonlinear algebraic equation. We already used a modulated transformer for a model of the slider crank mechanism (see Figures 4.6 and 4.7). However, in that case, the transformer is modulated by a kinematic displacement, which is a state variable needed to describe the system state. On the contrary, in Figure 4.21a, the transformer is modulated by a *power* variable. This is not merely a hypothetical possibility. Consider the bond graph displayed in Figure 4.22. It represents a simplified model of a series motor in which the inductances of the field and the armature coils have been neglected [31]. Let r denote the ratio of the gyrator. Then, the following equations are obtained from the bond graph.

$$M = r \times i \tag{4.42a}$$
$$r = f\,(i) \tag{4.42b}$$
$$u = r \times \omega \tag{4.42c}$$
$$i = \frac{1}{R}\,(\,E(t) \,-\, u\,) \tag{4.42d}$$

Due to hysteresis and saturation, $f()$ is a nonlinear function such that the current i is determined by an implicit nonlinear relation. If the inductances of the coils are taken into account by adding an I element to the 1-junction, then the algebraic loop disappears.

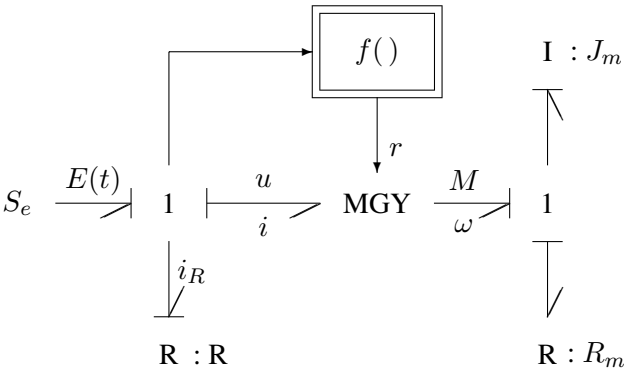

Fig. 4.22 Simplified bond graph of a series motor

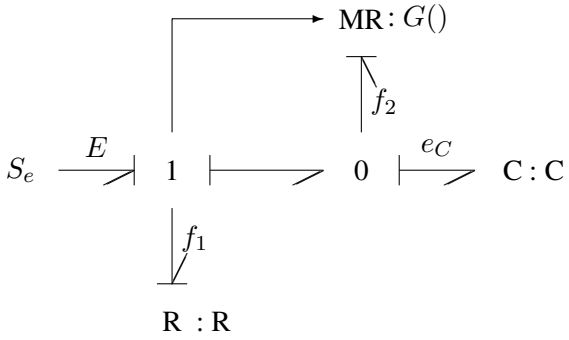

Fig. 4.23 Internal modulation without algebraic loop

Internal modulation does not necessarily result in algebraic loops. For illustration, we interchange the resistor and the C element in Figure 4.21b (cf. [12]). From the modified bond graph (Figure 4.23), we obtain the equations

$$f_1 = \frac{1}{R}\,(\,E\,-\,e_C\,) \tag{4.43a}$$

$$f_2 = G\,(\,e_C, f_1\,) \tag{4.43b}$$

$$\dot{e}_C = \frac{1}{C}\,(\,f_1\,-\,f_2\,)\,. \tag{4.43c}$$

Substitution of the output variables of the resistors into the equation of the energy store yields a state equation without algebraic constraint.

The examples of Figure 4.21 show that internal modulation may lead to algebraic loops that are not detected by inspecting causal paths alone. In addition, signals must also be taken into account that originate from junctions and modulate bond graph elements. On the other hand, internal modulation does not necessarily result in algebraic loops as the bond graph of Figure 4.23 illustrates. It is this possibility of algebraic loops not expressed by causal paths that explains why at the beginning of this chapter sources, transformers and gyrators have only been allowed to be modulated by state variables or system inputs. Finally, let us consider an example with an internally modulated source depicted in Figure 4.24. Since there is no causal path between resistors, the bond graph at a first glance suggests that the mathematical model can be reduced to state space form. From the bond graph of Figure 4.24, the following three algebraic equations for the controlled source and the two resistors and an ODE for the C energy store can be written.

$$u = k\,i_2 \tag{4.44a}$$

$$i_2 = \frac{1}{R_2}\,(\,u\,-\,u_C\,) \tag{4.44b}$$

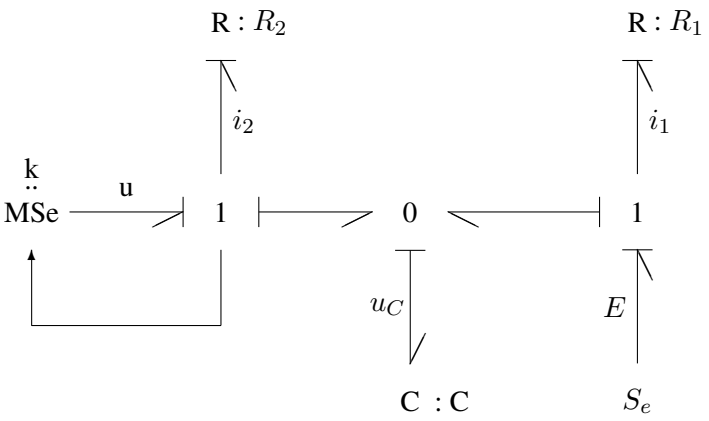

Fig. 4.24 Bond graph with an internally modulated source

$$i_1 = \frac{1}{R_1}\,(\,E\,-\,u_C\,) \tag{4.44c}$$

$$\dot{u}_C = \frac{1}{C}\,(\,i_1\,+\,i_2\,) \tag{4.44d}$$

In the example of the voltage follower (Figure 3.22), the output of the controlled source is proportional to the difference of the input voltage. The voltage across the capacitor is a state variable. In this example, the output of the controlled source is proportional to the power variable i_2. By taking into account the signal modulating the left-hand side source, we see that there is a flat loop between the controlled source and the resistor with resistance R_2. Apparently, if the source was independent, then there would be no algebraic loop associated with the causal path between the source and the resistor R_2. Substituting the constitutive equation of the controlled source into the equation of the resistor R_2 yields an equation that determines the controlling signal i_2.

$$R_2\,i_2 \;=\; k\,i_2 \;-\; u_C \tag{4.45}$$

Equation 4.45 is just the sum of all efforts at the left 1-junction. It is solvable for i_2 if $k \neq R_2$. Under this condition, the equations derived from the bond graph can be reduced into one state equation for u_C. In case $k = R_2$, the DAE system is of index one (The algebraic constraints need to be differentiated once in order to obtain $\dot{u}_C(t) = 0$. For $k = R_2$, the circuit degenerates into one with no dynamic element). The simple example shows that conclusions with regard to the form of the mathematical model cannot be drawn from considering causal paths alone if internal modulation is not excluded. The form of the mathematical model or the index of a DAE system may even depend on parameter values.

In [12], Cornet and Lorenz show how causality assignment and causality propagation can be used to establish a set of sorted equations in the sense of a compu-

tational order. Since algebraic loops prevent a complete sorting, their detection is essential in this context.

Breedveld argues that internal modulation should be relinquished from a conceptional point of view because basic features of elements can be changed and elements with arbitrary characteristics can be constructed by means of internal modulation [7]. Thus, there would be a potential risk that modelling violates physical conservation laws. Fundamental features of physical modelling would not be guaranteed any more. Van Dijk proposes to use a multiport with appropriate nonlinear constitutive equations instead of local internal modulation [32] where possible. He considers internal modulations as an exception.

4.9 The Method of Relaxed Causalities

So far, we have only used the standard procedure of Karnopp and Rosenberg for assigning and propagating computational causalities in bond graphs. Resulting causal patterns and their implication with regard to the form of the mathematical model have been analysed. The notion of the causal path has been essential in this context. In addition to the standard sequential causality assignment procedure SCAP, some modifications of this procedure have been proposed in the bond graph literature. In the following, first, the so-called *method of relaxed causalities* introduced by Joseph and Martens [20] is considered by means of the example of a hydraulic bridge (Figure 3.26).

In this example, the necessity appears to choose causality at two of the four resistors leading to two separate causal paths (cf. Figure 4.2) and the requirement that the resistors must have an invertible characteristic. Otherwise, causality at two resistors would not be in accordance with their characteristic. This can be taken into account by establishing implicit nonlinear equations that can only be numerically solved by iteration. In [20], Joseph and Martens propose a modification of the SCAP that enables one to assign nonlinear resistors the causality their characteristic requires and that allows violations at 0- and 1-junctions. For instance, if all resistors of the hydraulic bridge require conductance causality and if these causalities are assigned in the order R_1, R_2, R_3, R_4, then no causal paths appear, but at the lower right side 0-junction and at the upper left side 1-junction, causality rules cannot be maintained any longer. There are two type of conflicts highlighted by a flash. At the 0-junction, there is no effort that determines the effort at the other adjacent bonds. At the 1-junction, there are two flows that want to determine the common flow at all bonds (cf. Figure 4.25). If a source requires a causality at a resistive port that is not in accordance with the resistors constitutive relation, then the method of relaxed causalities enables one to insert an extra 0- or 1-junction and to reassign causality at the resistive port resulting in a causal violation at the junction as depicted in Figure 4.26. If the causality at a resistive port is determined by the preferred integral causality of an energy store and if the resistor characteristic requires reverse

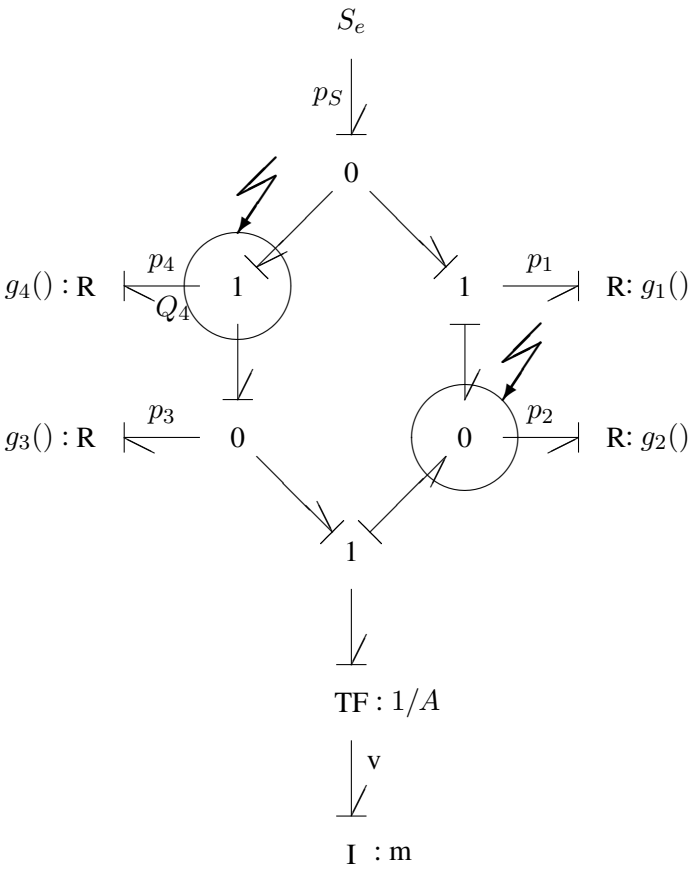

Fig. 4.25 Bond graph with two types of causal conflicts at a 0- and a 1-junction

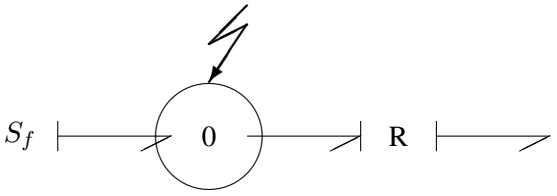

Fig. 4.26 Bond graph fragment with an extra 0-junction taking a causal violation

causality, then either the causality of the storage port can be changed into derivative causality or an extra junction can be included.

As the example of the hydraulic bridge shows, two types of causal violations at 0- and 1-junctions can be distinguished. Moreover, if several bonds want to determine

the common variable of a junction, Joseph and Martens have introduced a degree that indicates how many algebraic constraints must be established for each a junction in addition to the ODEs of the energy stores. That is, the resulting mathematical model is a DAE system.

Definition 4.18 (*Causal conflict of type 1*)**.** In this case, there is no bond that determines the common variable of the junction. At a 1-junction, the causal stroke of all adjacent bonds point towards the 1-junction. At a 0-junction, the causal stroke at all adjacent bonds is pointing away from the junction (Figure 4.27).

Definition 4.19 (*Causal conflict of type 2 and degree k*)**.** If there are $k+1$ bonds that want to determine the common variable of a junction, then there is a causal conflict of type 2 and degree k. That is, at a 1-junction, not one but $k+1$ flows are input to the junction, while at a 0-junction, $k+1$ instead of only one single effort are input to the junction (Figure 4.28).

According to these definitions, the bond graph of Figure 4.25 shows a causal conflict of type 1 at the right side 0-junction and a causal conflict of type 2 and degree 1 at the left side 1-junction.

If there is a causal conflict of type 1 at a 0-junction, then the effort at one of its adjacent bonds must be chosen as an input variable. Preferably, a bond is chosen that connects the 0-junction to a nonlinear resistive port with conductance causality or a port of an I energy store with preferred integral causality. Joseph and Martens call such a variable an *algebraic state variable*. In the example of the hydraulic bridge (Figure 4.25), the effort p_2 is chosen and considered to be an input to the 0-junction. Adding up the flows at that junction yields an equation that determines the algebraic state variable p_2.

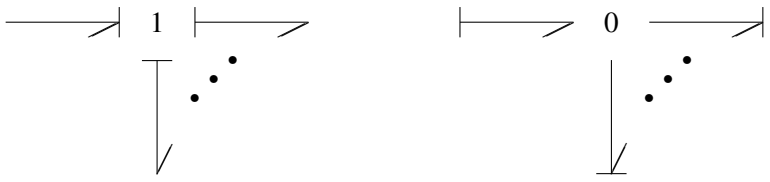

Fig. 4.27 Causal conflict of type 1

Fig. 4.28 Causal conflict of type 2 and degree k

$$0 \;=\; g_1\,(p_S \;-\; p_2) \;-\; g_2\,(p_2) \;+\; A\,v \tag{4.46}$$

If there is a causal violation of type 2 and degree k at a 0-junction with n adjacent bonds, and if none of the efforts of the adjacent bonds is a state variable, then an effort is arbitrarily chosen as an input to the 0-junction from those bonds that connect the junction to a nonlinear resistive port. Without loss of generality, e_1 is assumed to be that input. From the n flows at the 0-junction adding up to zero, flows $f_{k+2}, \ldots, f_n$ of those bonds causing no violation can be expressed by components of the state vector $\mathbf{x}$. That is, the flow f_1 into the resistive port can be represented in terms of the algebraic state variables $f_2, f_3, \ldots, f_{k+1}$ and the state vector $\mathbf{x}$. Hence, the constitutive equation of the resistive port takes the form

$$e_1 = \Psi_1\,(f_2, f_3, \ldots, f_{k+1}, \mathbf{x})\;. \tag{4.47}$$

In addition, for each of the k bonds $(2, \ldots, k{+}1)$ that want to determine the common effort of the 0-junction like bond 1 and that are causing a violation in this way, an equation of the form

$$0 \;=\; e_i \;-\Psi_i\,(f_i), \qquad\qquad i \;=\; 2, \ldots, k+1 \tag{4.48}$$

holds. Since there is a common effort at all bonds of a 0-junction, Equation 4.47 can be substituted into Equation 4.48. The result is a set of k implicit algebraic equations determining the algebraic state variables $f_2, \ldots, f_{k+1}$. Apparently, if e_1 is a state variable, then Equation 4.47 is not applicable.

Similar equations can be formulated for 1-junctions as their functionality is dual to that of 0-junctions.

In the case of a type 1 causal violation at a 1-junction, there is no flow that is input into the junction. Consequently, one flow must be chosen as an input. Effort continuity of the 1-junction provides an algebraic equation that determines the chosen input flow.

For causal violation of type 2 and degree k at a 1-junction, algebraic constraints corresponding to equations 4.47 and 4.48 are obtained for those flow variables that inflict causal violations. Consider the bond graph of Figure 4.25. From the two flows Q_4 and Q_5 that want to determine the common flow at the upper left 1-junction, Q_5 is chosen as an input. It can be represented in terms of the state variable, v, and the effort, p_4, of that bond inflicting the causal violation.

$$Q_5 \;=\; g_3\,(p_S \;-\; p_4) \;+\; A\,v \tag{4.49}$$

For that bond causing the violation the algebraic relation

$$Q_4 \;=\; g_4\,(p_4) \tag{4.50}$$

holds. Since there is a common flow at a 1-junction, Equation 4.49 can be substituted into Equation 4.50. The result is an equation that determines the algebraic state variable p_4. In this example, the method of relaxed causalities yields two coupled nonlinear implicit algebraic constraints for the algebraic state variables p_4 and p_2

and an ODE for the inertia of the piston.

$$0 = g_1\,(\,p_S\,-\,p_2\,)\,+\,A\,v\,-\,g_2\,(\,p_2\,) \tag{4.51a}$$

$$0 = g_4\,(\,p_4\,)\,-\,g_3\,(\,p_S\,-\,p_4\,)\,-\,A\,v \tag{4.51b}$$

$$\dot{v} = \frac{1}{m}\,A\,[\,(\,p_S\,-\,p_4\,)\,-\,p_2\,] \tag{4.51c}$$

Again, the resulting DAE has the form of Equations 4.4a–4.4b.

This result can also be obtained by inserting additional energy stores into the bond graph. If C energy stores are attached to the 0-junctions in the lower part of the bond graph shown in Figure 4.25, then the causal conflicts vanish. The mathematical model derived from the modified bond graph has the form of an explicit state space model. If the state equation of each additional C energy store is multiplied by its capacitance and if the latter tended to zero, then the above Equations 4.51a and 4.51b are the result.

4.10 Lagrange Causalities

In Section 4.4, the well known example of a slider crank mechanism was used to illustrate that the mathematical model takes the form of a DAE system if there is a causal path in the bond graph between an independent and a dependent storage port. Since the rod, assumed to be massless, links the piston to the flywheel, there is a geometric constraint between the piston's displacement and the angular position of the crank. Apparently, the number of unknowns in Equation 4.25 is not minimal. The mechanism has only one degree of freedom. Moreover, the balance of moments depends on the angular position of the crank. It is a peculiarity of mechanical systems in planar or 3D motion that generally equations determining their dynamic equilibrium cannot be formulated without knowing geometric positions. In contrast, power variables in electrical systems must comply with Kirchhoff's laws that do not depend on generalised displacements, viz. charge or flux linkage. Furthermore, the complexity of mathematical models of mechanical systems strongly depends on the reference frame(s) in use and on the choice of the state variables. Therefore, often appropriate coordinates, so-called *generalised coordinates*, used in mechanics and equations of motion are formulated as Lagrange equations of the second kind. This way, a compact and, due to geometric constraints, a strongly nonlinear model results with a minimal number of state variables. These are displacements and velocities of the bodies chosen with respect to appropriate reference frames. Lagrange equations, however, are not confined to mechanical systems. Generalised coordinates are only special generalised displacements, but in the context of Lagrange equations of motion, the notion of generalised coordinates is kept even when this method of establishing equations of motion is used in non-mechanical energy domains. If a Lagrange approach is applied, for instance, to describe nonlinear electrical systems, then generalised coordinates are the integral of currents with respect to time (These

quantities are not necessarily the charge of certain capacitors). Karnopp has given a procedure that, first of all, enables one to identify generalised coordinates and their associated so-called *generalised forces* in a bond graph [23]. In a second step, the Lagrangian L is determined from the bond graph as a function of the generalised coordinates and their time derivatives. Proper derivatives of the Lagrangian then, eventually, yield the Lagrange equations.

In the following, we will see that as opposed to a DAE system, Lagrange equations can be *directly* derived from a bond graph. In order to identify the needed generalised coordinates, we use the modification of the standard sequential causality assignment procedure (SCAP) given by Karnopp in [23]. Further procedures for the derivation of Lagrange equations with Lagrange multipliers directly from a bond graph have been proposed by Bos [6], van Dijk [32] and Marquis-Favre and Scavarda [25].

4.10.1 Identification of Generalised Coordinates in a Bond Graph

1. All independent sources are assigned a causality according to their type. This causal information is propagated into the junction structure as far as possible. If any causal conflicts appear, modelling assumptions must be checked and the model must be modified.
2. If the common flow variable of a 1-junction is still undetermined, then an *artificial flow source* is attached that imposes a flow. This flow information is propagated into the junction structure as far as possible.
   If there are no undetermined 1-junctions left and if the bond graph is still causally incomplete, then a 1-junction is inserted into an acausal bond.
3. Step 2 is repeated until all bonds have a causal stroke.

The 1-junctions to which an artificial flow source has been attached represent the time derivatives of the generalised coordinates we are looking for. There is no rule as to which undetermined 1-junction an artificial flow source has to be attached to first. Moreover, if there are no undetermined 1-junctions but still acausal bonds, then an acausal bond can be arbitrarily chosen for insertion of a 1-junction. That is, the set of generalised coordinates identified by this procedure is not unique.

4.10.2 Determination of Generalised Forces from a Bond Graph

The generalised forces are the efforts into the artificial flow sources. They are obtained by adding the efforts at the 1-junction to which an artificial flow source has been attached. However, in this sum, only efforts from sources and resistors are taken into account. In order to ensure that the generalised force is the sum of all these efforts including their sign, the half arrow points toward the artificial flow source [23]. More precisely, one should talk of artificial flow sinks.

4.10.3 Derivation of Lagrange Equations from a Bond Graph

Lagrange equations can be directly derived from a bond graph by adding up the efforts at all 1-junctions that represent the time derivative of a generalised coordinate. In contrast to the procedure applied for identification of generalised forces, in this balance, all efforts are taken into account. The sum of all efforts into an artificial flow source is equal to zero. In the following, both steps shall be applied to the example of the slider crank mechanism and to an example of an electrical network.

Example: Slider Crank Mechanism

If an artificial flow source is attached to the 1-junction representing the angular velocity $\omega = \dot{\varphi}$, and if this flow information is propagated into the junction structure, then the bond graph is already causally complete after this step (Figure 4.29). That is, the angle φ is the only generalised coordinate according to the one degree of freedom of the mechanism (If we had attached an artificial flow source to the right-hand 1-junction, the displacement of the piston would have become the generalised coordinate). From the balance of efforts at the left-hand 1-junction

$$0 = M - J\ddot{\varphi} - \tilde{M} \tag{4.52}$$

we obtain the same second order ODE for φ

$$(J + T\,m\,T)\ddot{\varphi} + (T\,m\dot{T})\dot{\varphi} + (T\,r\,T)\dot{\varphi} = M + TF \tag{4.53}$$

that would result after establishing and proper differentiation of the Lagrangian.

In general

$$T^* := \int_0^f p(\tilde{f})\,d\tilde{f} \tag{4.54}$$

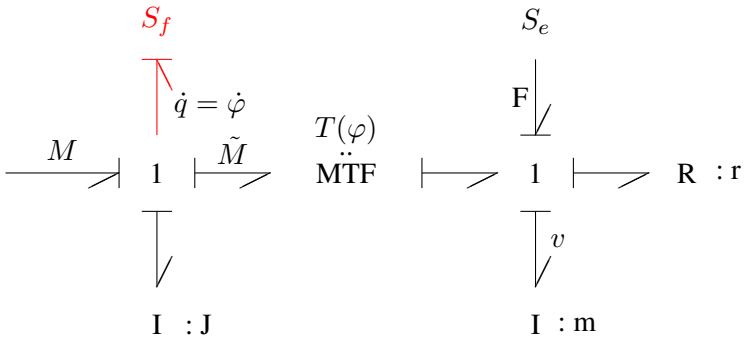

Fig. 4.29 Bond graph of the slider crank mechanism with an artificial flow source

denotes the *kinetic co-energy* and V the potential energy of a system. The Lagrangian is defined as the difference of both terms

$$L := T^* - V . \tag{4.55}$$

(The distinction between kinetic energy and kinetic co-energy is of relevance only for relativistic mechanics and for systems with non-mechanical, nonlinear inertias. Otherwise, $T^* = T$.) Let $\mathbf{q}$ denote the vector of generalised coordinates and $\mathbf{Q}$ the vector of generalised forces, then T^* is a function of $\mathbf{q}$ and $\dot{\mathbf{q}}$, whereas V is a function of $\mathbf{q}$ and

$$\frac{d}{dt}\frac{\partial L}{\partial \dot{\mathbf{q}}}(\mathbf{q}, \dot{\mathbf{q}}) - \frac{\partial L}{\partial \mathbf{q}}(\mathbf{q}, \dot{\mathbf{q}}) = \mathbf{Q} \tag{4.56}$$

is the Lagrange equation of motion. For the example of the slider crank mechanism, φ is the only generalised coordinate. The generalised force is $Q = M - T[r(T\dot{\varphi}) - F]$. The Lagrangian is the sum of the kinetic energy of the flywheel and of the piston.

$$L = \frac{1}{2}\left(J\,\dot{\varphi}^2 + m\,(T\dot{\varphi})^2 \right) \tag{4.57}$$

If L is differentiated according to Equation 4.56, then Equation 4.53 results.

Virtual Inertia and its Companion Gyristor

Section 3.4 mentions that in the case of an independent I energy store and a dependent I energy store coupled by a transformer with a constant ratio (Figure 3.14), the energy store with derivative causality can be transformed over the transformer and can be combined with the independent energy store. Since in Equation 4.53 the factor pre-multiplying $\ddot{\varphi}$ has the same form as the one in the bond graph of Figure 3.15, it is obvious to also represent Equation 4.53 by a bond graph. In the case of the slider crank mechanism, however, the modulus of the transformer is a function of the generalised coordinate φ. Consequently, the term $J + TmT$ viewed as moment of inertia, $\tilde{J}$, is not constant. In [3], Allan denotes $\tilde{J}$ as an *instantaneous* or *virtual inertia*. Unlike the case of a transformer with constant modulus, the consequence of this view is that the additional term $(Tm\dot{T})\,\dot{\varphi})$ must be represented by a new artificial bond graph element (GR) called *gyristor* by Allan. It takes into account that the virtual inertia depends on the displacement φ and, therefore, is not constant ($Tm\dot{T} = (1/2)\,\dot{\tilde{J}}$). The new element ensures that the kinetic co-energy of the virtual inertia is conserved. That is, it is equal to the kinetic co-energy of the mechanism [3]. If the new artificial element is accepted, then Lagrange equation (4.53) can be represented by the bond graph of Figure 4.30.

The derivation of Lagrange equations from a bond graph is suitable especially for mechanical systems with complicated kinematics if moving reference frames are used and for nonlinear systems. The resulting second order equations of motion are strongly nonlinear. The model, however, is much more compact than a DAE system. This has been illustrated by Karnopp in an article on different approaches to the derivation of equations from a bond graph by comparing the equations for the

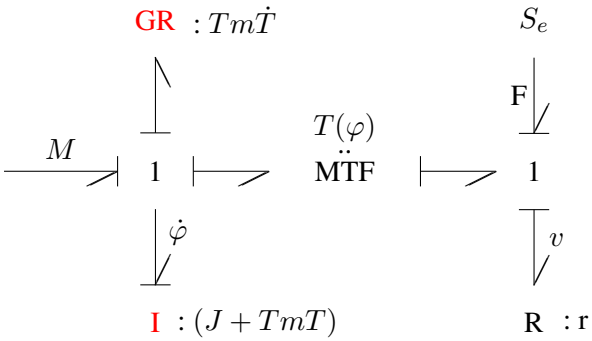

Fig. 4.30 Bond graph with virtual inertia and gyristor as companion

components of the momentum of a simple mathematical pendulum with respect to a fixed Cartesian reference frame to the well known second order equation for the angle [22].

Example: RLC Network

Finally, we will show by means of the simple RLC circuit of Figure 4.31 that the Lagrange method is not confined to mechanical systems. Application of Karnopp's method to the bond graph of the circuit yields the two generalised coordinates $\dot{q}_1$ and $\dot{q}_2$ (Figure 4.32).

In the next step, all efforts at the 1-junctions are added up assuming that the efforts into the artificial flow sources are zero. After differentiation of the effort balance at the left-hand 1-junction, the two Lagrange equations are

$$\frac{1}{C_1}\, I_e = R\,\ddot{q}_1 + \left(\frac{1}{C_1} + \frac{1}{C_2}\right) \dot{q}_1 - \frac{1}{C_2}\,\dot{q}_2 \tag{4.58a}$$

$$0 = L_1\,\ddot{q}_2 + \frac{1}{C_2}\, q_2 - \frac{1}{C_2}\, q_1 \,. \tag{4.58b}$$

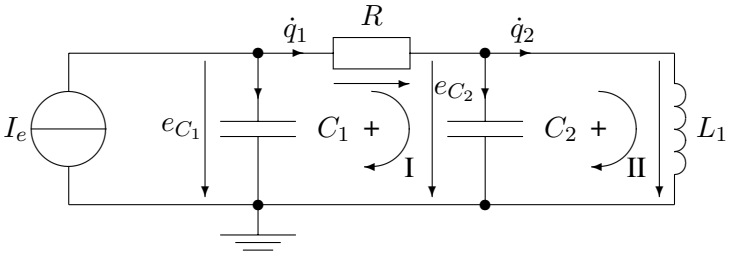

Fig. 4.31 RLC circuit

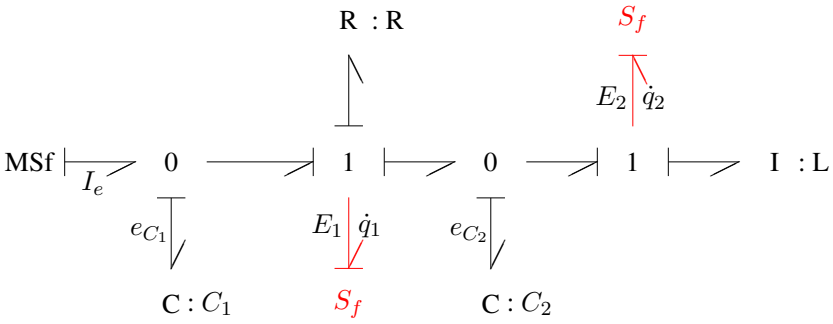

Fig. 4.32 Bond graph of the RLC circuit with artificial flow sources

Equation 4.58a can also be directly obtained from the network by adding up all voltages along mesh I, by differentiating this sum with respect to time and by using Kirchhoff's current law to express the currents into the capacitors by the derivatives of the generalised coordinates. Likewise, the second Equation 4.58b results from adding up all voltages along mesh II.

The same equations result if the Lagrangian of the system

$$L = \frac{1}{2} L_1 \dot{q}_1^2 - \frac{1}{2C_1} \left(\int_0^t (I_e(\tau) - \dot{q}_1) d\tau \right)^2 - \frac{1}{2C_2} (q_1 - q_2)^2 \tag{4.59}$$

is differentiated according to Equation 4.56. The generalised forces

$$E_1 = -R \dot{q}_1 \tag{4.60a}$$
$$E_2 = 0 \tag{4.60b}$$

are obtained from the bond graph of Figure 4.32.

4.11 Conclusion

In the previous chapter, the important notion of a causal path was introduced. In the process of a systematic derivation of a mathematical model from a causal bond graph, first, only causal paths between resistive ports had been allowed. In this chapter, different types of causal paths and their influence on the form of the mathematical model have been considered. The following zero-order causal paths have been analysed.

1. Causal paths between resistive ports
2. Causal paths between storage ports of the same type
3. Causal loops
4. Bond graphs with different types of causal paths

In these cases, a mathematical model of the form of a DAE system can be derived from the bond graph. If this form is not supported by the available simulation program or if an explicit state space form is needed for other reasons, then causal paths can be removed by inserting additional energy stores or resistors.

In the case of *linear* algebraic constraints, one may try to remove them by symbolic manipulation supported by various algebra programs. The first approach is generally applicable and can be justified from a physics point of view by taking into account effects that are negligible with regard to the overall dynamics of a system. For instance, in multibody systems, joints linking bodies are not completely rigid, but have got some compliance and exhibit some dissipation. Consequently, inertias of bodies can be decoupled by a spring-damper pair. The disadvantage, however, is that fast transients or high frequency oscillations are introduced that are not significant for the overall system dynamics.

Transients or oscillations in a system considered to be isolated can be identified by looking at causal paths between a storage port and a resistive port and between storage ports of different type. For linear or linearised characteristics, time constants or natural frequencies can be obtained from element parameters. Since transients and oscillations in a system are not isolated but influence each other, this approach yields only a rough estimate of the actual time constants and natural frequencies of the linearised system which is not so bad because determination of eigenvalues is so costly that their evaluation prior to simulation is not worthwhile.

Inserting additional energy stores or resistors often results in a stiff ODE system. Numerical solution of such system requires an implicit stiffly stable integration method. Thus, the solution is costly with regard to computational time in comparison to an explicit method. Moreover, including additional energy stores increases the order of the ODE system. The disadvantage of a symbolic reduction approach is that it is not generally applicable.

The standard sequential causality assignment procedure, SCAP, may lead to the requirement of inverting the characteristic of some resistive ports. If that is not possible for a resistive port, causality in the bond graph is not in accordance with the form of constitutive relation. In this case, the equation of a port can be considered an implicit non-invertible algebraic relation for the determination of the output variable. A transformation of the DAE system into a state space model is not possible.

An alternative to the standard SCAP is the method of relaxed causalities introduced by Joseph and Martens. Following this procedure, nonlinear resistive ports always obtain the causality corresponding to their constitutive relation with the consequence of possible causal violations at 0- or 1-junctions. The type of causal violation indicates how many algebraic constraints must be formulated for each such junction. Hence, in general, the procedure of Joseph and Martens yields mathematical models of the form of a DAE system. Consequently, causal conflicts do not necessarily indicate contradictions in the model, meaning that the model equations cannot be solved. Whether a mathematical model can be reduced to an explicit state space model depends on whether the algebraic constraints resulting from causal violations at 0- or 1-junctions can be symbolically solved.

If there is a causal path between an independent and a dependent linear energy 1-port store, then both energy stores can be combined into one with integral causality. Transforming an energy I store with derivative causality over a transformer requires its parameter to be multiplied by the square of the transformer modulus. If the modulus is controlled by a generalised displacement, then the result is a so-called virtual inertia that has an artificial element, the gyristor, as a companion. The latter takes into account that the virtual inertia depends on the instantaneous value of the generalised displacement and ensures that the kinetic co-energy of the virtual inertia is conserved [3].

Another option is to apply a procedure introduced by Karnopp that enables one to identify generalised coordinates in a bond graph and to derive Lagrange equations for them. This can be achieved by adding all efforts at the 1-junctions representing the derivatives of generalised coordinates. The method of Lagrange equations is not confined to mechanical systems even if the terminology originating from mechanics is retained. For electrical systems, the charge of capacitors can be used as generalised coordinates. In any case, the result is a compact generally nonlinear model with a minimal number of state variables.

If the mathematical model derived from a bond graph takes the form of a DAE system, then its index is an important characteristic with regard to the numerical solution. Van Dijk has shown that conclusions with regard to the index can be drawn from inspection of causal patterns in the bond graph. For instance, if causal paths occur between resistive ports or between independent and dependent storage ports, then the DAE system for the outputs of the energy stores is of index one.

For bond graphs with causal loops (Definition 3.10), Andry and Rosenberg have shown that the algebraic equations of the general junction structure (Definition 2.14) are solvable if and only if causal loops are pairwise disjoint and if for each causal loop, its loop gain (Definition 4.16) is different from $+1$. If causal paths between independent and dependent storage ports share bonds with causal loops while causal loops do not touch, then the DAE system is of index > 1, as has been shown by van Dijk. Consequently, solvers based on the BDF method, like the widely used DASSL code, cannot be used, in general, for such DAE systems.

Causal loops of unity loop gain in the junction structure are an indication of a weak point of the SCAP. In the bond graph of Figure 4.16, the fixed causality of the flow source and the preferred causalities of the I energy stores do not propagate into the junction structure. According to the SCAP, causality must be chosen at a resistor. If conductance causality is assigned, a causal conflict results at a 0-junction. On the contrary, assignment of resistance causality leaves the bond graph causally incomplete. Hence, causality must be chosen at an internal bond. No matter at which of the six internal bonds causality is chosen, the result is a causal loop of unity loop gain. Setting up equations reveals that the causal loop of unity loop gain as well as the causal conflict at the 0-junction indirectly express a nodicity property of the delta subnetwork of resistors. According to this nodicity property, the currents of the source and of the two I energy stores cannot be independent in contrast to the assignment of preferred causalities at the storage ports. The nodicity property can be expressed in the bond graph by assigning derivative causality to one of the

two I energy stores. As a result, the causal loop disappears. In the bond graph of Figure 4.18, the equation of cut-set 1 depicted in the network of Figure 4.15 is not expressed directly, but the bond graph is consistent with that constraint. In that light, the weakness of the SCAP could be accepted. With regard to the numerical solution of the DAE system, however, it turns out that it is of index > 1. If one of the two I energy stores obtains derivative causality, then the DAE system is of index one, allowing for a safe numerical solution. Van Dijk has proposed a modification of the SCAP that avoids the emergence of causal loops of unity loop gain such that bond graphs causally completed this way lead to DAE systems of lower index.

Finally, internal modulation may cause algebraic loops. They are not expressed by causal paths alone. Their systematic detection is not so easy. Since internal modulation enables the representation of functional relations that do not comply with physical conservation laws, Breedveld suggests to refrain from using it.

References

[1] DASPK. URL http://www.cs.ucsb.edu/~cse/software.html.
[2] Octave. URL http://www.gnu.org/software/octave/.
[3] R.R. Allen. Multiport Representation of Inertia Properties of Kinematic Mechanisms. *Journal of the Franklin Institute*, 308(3):235–253, 1979.
[4] W. Borutzky. Kausalitäten in Bond-Graphen und Formen mathematischer Systemmodelle – Eine bewertende Untersuchung. In D. Tavangarian, editor, *Simulationstechnik, 7. Symposium in Hagen, September 1991*, pages 505–509. Vieweg Verlag, 1991.
[5] W. Borutzky. On Interrelations Between Bond Graph Causal Patterns and the Numerical Solution of the Mathematical Model. In J.J. Granda and F.E. Cellier, editors, *International Conference on Bond Graph Modeling, ICBGM'93, Proc. of the 1993 Western Simulation Multiconference*, pages 93–100. SCS Publishing, January 17–20 1993. Simulation Series, voulume 25, No. 2, ISBN: 1-56555-019-6.
[6] A.M. Bos. *Modelling Multibody Systems in Terms of Multibond Graphs with Application to a Motorcycle*. PhD thesis, Univ. of Twente, Enschede, The Netherlands, 1986.
[7] P.C. Breedveld. *Physical Systems Theory in Terms of Bond Graphs*. PhD thesis, Univ. of Twente, Enschede, The Netherlands, 1984.
[8] K.E. Brenan, S.L. Campbell, and L.R. Petzold. *Numerical Solution of Initial-Value Problems in Differential-Algebraic Equations*. North-Holland, 1989.
[9] A.P.J. Breunese. *Automated support in mechatronic systems modeling*. PhD thesis, Univ. of Twente, Enschede, The Netherlands, 1996.
[10] F.T. Brown. Direct Application of the Loop Rule to Bond Graphs. *Journal of Dynamic Systems, Measurement and Control*, pages 253–261, September 1992.
[11] S.L. Campbell, J.Ph. Chancelier, and R. Nikoukhah. *Modeling and Simulation in Scilab/Scicos*. Springer Science+Business Media, New York, NY, U.S.A., 2006.
[12] A. Cornet and F. Lorenz. Equation Ordering Using Bond Graph Causality Analysis. In P.C. Breedveld et al., editor, *Modelling and Simulation of Systems*, pages 55–58. J.C. Baltzer AG, Scientific Publishing Co., 1989.
[13] P.J. Gawthrop and L. Smith. *Metamodelling: Bond Graphs and Dynamic Systems*. Prentice Hall International (UK) Limited, Hemel Hempstead, 1996. ISBN: 0-13-489824-9.
[14] C. W. Gear. Differential-algebraic equation index transformations. *SIAM J. Sci. Stat. Comput.*, 9(1):39–47, 1988.

[15] C.W. Gear and L.R. Petzold. Ode methods for the solution of differential/algebraic systems. *SIAM J. Numer. Anal.*, 21:367–384, 1984.

[16] E. Griepentrog and R. März. *Differential-Algebraic Equations and Their Numerical Treatment*, volume 88. Teubner, 1986.

[17] E. Hairer and G. Wanner. *Solving Ordinary Differential Equations II, Stiff and Differential-Algebraic Problems*. Springer-Verlag, 2^{nd} edition, 1996.

[18] E. Hairer, C. Lubich, and M. Roche. *The Numerical Solution of Differential-Algebraic Systems by Runge-Kutta Methods*. Number 1409 in Lecture Notes in Mathematics. Springer-Verlag, 1989.

[19] N. Hogan and E.D. Fasse. Conservation principles and bond graph junction structures. In *Proc. ASME Winter Anual Meeting, Automated Modeling for Design*, volume DSC-8, pages 9–13. ASME, 1989. New York.

[20] B.J. Joseph and H.R. Martens. The Method of Relaxed Causality in the Bond Graph Analysis of Nonlinear Systems. *Trans. ASME Journal of Dynamic Systems, Measurement, and Control*, 96:95–99, 1974.

[21] Th. Kailath. *Linear Systems*. Englewood Cliffs, N. J., USA, 1980.

[22] D.C. Karnopp. Alternative Bond Graph Causal Patterns and Equation Formulations for Dynamic Systems. *Journal of Dynamic Systems, Measurement, and Control*, 105:58–63, 1983.

[23] D.C. Karnopp. Lagrange's Equations for Complex Bond Graph Systems. *ASME Journal of Dynamic Systems, Measurement, and Control*, 99(4):300–306, December 1977.

[24] D.G. Luenberger. Dynamic equations in descriptor form. *IEEE Transactions Automatic Control*, 22:312–321, 1977.

[25] W. Marquis-Favre and S. Scavarda. A procedure for generating the Lagrange equations from the bond graph representation using the λ-multiplier method. In J.J. Granda and F.E. Cellier, editors, *Proc. of the 1999 International Conference on Bond Graph Modeling and Simulation*, volume 31 (1), pages 263–268, 1999.

[26] J.R. Ort and H.R. Martens. The Properties of Bond Graph Junction Structure Matrices. *Journal of Dynamic Systems, Measurement, and Control*, 95:362–367, 1973.

[27] L. Petzold. Differential/algebraic equations are not ode's. *SIAM J. SCI STAT COMPUT*, 3(3): 367–384, 1982.

[28] R.C. Rosenberg and A.N. Andry. Solvability of Bond Graph Junction Structures with Loops. *IEEE Trans. on Circuits and Systems*, CAS-26(2):130–137, February 1979.

[29] Scilab Consortium. Scilab. URL http://www.scilab.org/.

[30] S.Li and L. Petzold. Design of New DASPK for Sensitivity Analysis. Technical report, UCSB, 1999. URL http://www.engineering.ucsb.edu/~cse/.

[31] J.U. Thoma. *Introduction to Bond Graphs and their Appliations*. Pergamon Press, Oxford, 1975.

[32] J. van Dijk. *On the role of bond graph causality in modelling mechatronic systems*. PhD thesis, Univ. of Twente, Enschede, The Netherlands, 1994.

[33] J. Won and N. Hogan. Nodic and Non-Nodic Structures in Physical Systems. In J.J. Granda and F.E. Cellier, editors, *ICBGM'99, 4th International Conference on Bond Graph Modeling and Simulation*, pages 90–95. SCS Publishing, 1999. Simulation Series, volume 31, No. 1, ISBN: 1-56555-155-9.